



Enhanced multi-objective Evolutionary Mating Algorithm with improved crowding distance and Levy flight for optimizing comfort index and energy consumption in smart buildings

Muhammad Naim Bin Nordin ^a , Mohd Herwan Sulaiman ^{a,c,*} , Nor Farizan Zakaria ^a,
Zuriani Mustafa ^b 

^a Faculty of Electrical & Electronics Engineering Technology, Universiti Malaysia Pahang Al-Sultan Abdullah, 26600 Pekan Pahang, Malaysia

^b Faculty of Computing, Universiti Malaysia Pahang Al-Sultan Abdullah, 26600 Pekan Pahang, Malaysia

^c Centre for Research in Advanced Fluid & Processes (Fluid Centre), Universiti Malaysia Pahang Al-Sultan Abdullah, Gambang Campus, 26300 Kuantan, Pahang, Malaysia

ARTICLE INFO

Keywords:

Comfort index optimization
Crowding distance
Energy efficiency
Evolutionary Mating Algorithm
Levy flight
Multi-objective optimization
Pareto optimization
Smart buildings

ABSTRACT

This paper introduces a novel Multi-Objective Evolutionary Mating Algorithm (MOEMA) designed to address the inherent challenges of optimizing comfort index and energy consumption in smart building systems. While current Evolutionary Mating Algorithms (EMA) primarily focus on single-objective optimization and rely on weighted functions for handling multiple objectives, such approaches prove impractical for the complex trade-offs between comfort index and energy efficiency. The proposed MOEMA enhances the original EMA framework through two key innovations: an improved crowding distance function inspired by the Non-dominated Sorting Genetic Algorithm (NSGA) to enhance solution diversity and selection pressure, and the integration of Levy flight mechanics to improve exploration efficiency by balancing local and global searches. These enhancements enable MOEMA to effectively navigate complex multi-objective landscapes, leading to more diverse and well-converged Pareto-optimal solutions. The algorithm's performance is thoroughly assessed using the chosen benchmark functions and validated through practical applications in smart building environments. It simultaneously optimizes various comfort parameters, including temperature, illuminance, and air quality, while minimizing energy consumption and maximizing the comfort index. Comparative analysis against established algorithms, like NSGA-II demonstrates MOEMA's effectiveness in achieving superior solution diversity and convergence characteristics. The results indicate that MOEMA offers a robust framework for handling the complex balance between the smart building's comfort index and energy usage where it achieves 0.03 % better at comfort index and with 10.65 % lower energy consumption than NSGA-II. It contributing to the broader fields of building automation and sustainable development while aligning with Industry 4.0 initiatives.

1. Introduction

Multi-objective optimization remains a critical challenge across various scientific and engineering domains, particularly in scenarios characterized by conflicting objectives [1]. This challenge is especially significant in smart building systems, where optimizing both the comfort index and energy consumption involves inherently competing goals. Several studies have explored this issue. For instance, a recent study applied a multi-objective optimization approach to optimize Venetian blinds in office buildings, significantly reducing energy consumption by

40–50 % while improving both visual and thermal comfort, demonstrating the effective use of multi objective like Non-dominated Sorting Genetic Algorithm II (NSGA-II) in balancing energy efficiency and occupant comfort [2]. The study demonstrates the practical effectiveness of multi-objective algorithms like NSGA-II in balancing energy efficiency and occupant comfort, reinforcing the relevance of multi-objective optimization techniques in smart building environments. Similarly, a sequential optimization approach has been demonstrated as an effective and computationally efficient method for handling multiple objectives, optimizing thermal comfort and energy

* Corresponding author.

E-mail addresses: naimnordin0105@gmail.com (M.N.B. Nordin), herwan@umpsa.edu.my (M.H. Sulaiman), norfarizan@umpsa.edu.my (N.F. Zakaria), zuriani@umpsa.edu.my (Z. Mustafa).

<https://doi.org/10.1016/j.fraope.2025.100286>

Received 4 January 2025; Received in revised form 29 March 2025; Accepted 27 May 2025

Available online 1 June 2025

2773-1863/© 2025 The Author(s). Published by Elsevier Inc. on behalf of The Franklin Institute. This is an open access article under the CC BY-NC-ND license (<http://creativecommons.org/licenses/by-nc-nd/4.0/>).

demand in building performance design, and achieving a 91.2 % reduction in computational effort compared to traditional full factorial searches [3]. The importance of computational efficiency in real-world applications directly aligns with the motivation to develop an algorithm that balances comfort and energy consumption while improving convergence efficiency.

Moreover, one method integrates a multi-objective evolutionary algorithm with surrogate models to optimize building energy use and thermal comfort while lowering computational costs [4]. The approach emphasizes the necessity of balancing algorithmic complexity and performance, a key consideration in the development of multi-objective optimization method. Similarly, research optimizing healthy buildings considers factors including energy usage, air quality, and aesthetic comfort [5], illustrating smart buildings' multi-faceted optimization challenges. An improved NSGA-II provides the theoretical foundation for a building design model that enhances both comfort and energy efficiency through Pareto solutions [6]. The study demonstrates NSGA-II's application in green building design. While NSGA-II remains widely used for multi-objective optimization, its limitations in solution diversity and convergence necessitate research for algorithmic improvements. In addition, NSGA-II combined with machine learning has been used to optimize, assess, and predict light, energy use, and thermal comfort in educational building lifts [7]. Furthermore, a recent study integrates Radial Basis Function (RBF) neural networks with the NSGA-II algorithm and Nearest Neighbor Component Analysis (NCA) to create a comprehensive NCA-GA-RBF neural network approach. This technique optimizes Passive House designs in China by generating financially feasible solutions while simultaneously reducing occupant discomfort hours and overall energy demand [8].

In addition to multi objective optimization related to energy and comfort, a recent study on radiant floor heating in a net Zero Energy House achieved an 11.6 % energy reduction while maintaining thermal comfort via multi-objective optimization [9]. Similarly, research on Phase Change Materials (PCM) in hospital walls improved thermal comfort by 37–43 % and reduced energy demand by nearly 8 % [10]. The study highlights the necessity of considering comfort-related parameters alongside energy efficiency, reinforcing the multi-objective nature of the problem. Recent research also highlights the importance of intelligent multi-objective optimization methods, like genetic algorithms and particle swarm optimization, in balancing energy use and comfort factors in smart buildings, improving occupant well-being and energy efficiency [11,12].

Furthermore, a study utilized a Multi-Objective Grey Wolf Optimizer (MOGWO) to optimize energy consumption schedules in residential environments. By integrating renewable energy systems, the research achieved improved energy efficiency and cost reduction while preserving user comfort levels [13]. This further emphasizes the role of advanced metaheuristic algorithms in smart energy management, aligning with the goals of this paper. Furthermore, A smart home energy management study employed a multi-objective improved Biogeography-Based Optimization (IBBO) algorithm to optimize appliance scheduling. By simultaneously minimizing electricity costs and peak-to-average ratio, the research reduced operational costs and peak loads, outperforming other optimization methods like Grey Wolf Optimizer (GWO) and Whale Optimization Algorithm (WOA), emphasizing the potential of multi-objective optimization in smart home energy management [14]. Despite these advancements, significant limitations persist in addressing truly multi-objective optimization scenarios. A primary challenge lies in effectively balancing the delicate trade-offs on the Pareto front between maintaining optimal comfort levels and minimizing energy consumption.

Instead of multi-objective optimization, single objective optimization has also addressed this issue. This is evident in the Bat Algorithm (BA), Evolutionary Mating Algorithm (EMA), and its variations, which have been suggested to maximize the comfort index and reduce energy consumption at the same time [15–17]. Nevertheless, single-objective

optimization is often unsuitable for problems requiring trade-offs between competing goals, as it simplifies complex relationships into a single measure using arbitrary weightings. In the field of single objective optimization to solve the electricity consumption issue, this also can be seen in other study that employs single-objective optimization to derive optimal strategies for specific aspects of electricity supply chain management, such as minimizing electricity consumption costs or maximizing the Green Energy Coefficient (GEC), within a multi-period stochastic framework [18]. In this problem, the cost function reduces the problem to a single objective, but it requires pre-defined weights for the trade-offs. Multi-objective optimization gives designers richer information, allowing them to make better compromise choices, whereas single objective optimization offers a direct solution for a given objective [19].

Moreover, some studies rely on parametric analysis or energy conservation approaches instead of formal optimization tools. For example, comparative analysis has been used to identify the best-performing strategies for balancing comfort and energy efficiency, but such methods lack the rigorous exploration capabilities of multi-objective optimization algorithms [20]. Similarly, energy conservation measures, such as advanced glazing and LED lighting, have been explored in [21], aligning with official building guidelines. While effective, these strategies do not provide optimal configurations when multiple conflicting objectives are involved.

As demonstrated in recent studies of building performance, managing multiple competing objectives poses significant challenges. For example, optimizing occupant comfort through cooling systems or building envelope modifications often increases energy consumption [22]. Conversely, strict energy reduction strategies may compromise comfort levels. This trade-off highlights the necessity of multi-objective optimization approaches capable of systematically balancing these competing objectives. Moreover, recent studies [23], emphasize that resource consumption in buildings is influenced by both operational decisions and user behavior, further complicating optimization efforts.

Beyond building scenarios, multi-objective approaches have also been widely applied in various fields beyond. For instance, the concept has been utilized in Cyber-Physical Power Systems (CPPSs) to model stealthy False Data Injection Attacks (FDIA) as a multi-objective optimization problem. The approach optimizes both the minimization of contaminated measurements and maximization of the attack impact, solved using NSGA-II [24]. This highlights the flexibility of multi-objective algorithms in addressing complex trade-offs in different domains. Other than that, multi-objective optimization has been applied in deep learning models for SAR image classification, where a robust convolutional neural network (MoAR-CNN) was developed to optimize the trade-off between clean accuracy and adversarial robustness. The study introduced NSGA-II to automatically search for optimal neural architectures and hyperparameters, showcasing the adaptability of NSGA-II in optimizing diverse problem spaces [25].

In the field of optimization, the increasing complexity of real-world problems has driven the demand for algorithms capable of balancing multiple conflicting objectives. Numerous single objective algorithms have recently been developed and enhanced with specialized operators to effectively handle multi-objective problems. Notable examples include the MOGWO [26], Multi-Objective Ant Lion Optimizer (MALO) [27], and Multi-Objective Grasshopper Optimization Algorithm (MOGOA) [28], among others. Nature-inspired algorithms have gained prominence in tackling multi-objective optimization challenges due to their robustness and ability to explore complex solution landscapes. Among these, Particle Swarm Optimization (PSO) [29] and GA [30] have been extensively applied. PSO mimics social behavior patterns in bird flocks and fish schools, while GA emulates biological evolution through selection, crossover, and mutation—both effectively evolving populations of solutions toward optimality. However, despite their success, traditional nature-inspired algorithms often struggle with maintaining diversity among solutions and efficiently converging to the Pareto front, especially in high-dimensional and highly conflicting

objective spaces [31]. The additional information about various multi-objective applications and utilising algorithms inspired by nature helps researchers in developing new algorithms or improving existing ones.

The optimization principle of the No Free Lunch (NFL) theorem, proposed by Macready and Wolpert [32] emphasizes the continuous need for novel algorithmic approaches. It demonstrates that not every optimization problem can be resolved by a single optimization algorithm, thereby encouraging researchers to create fresh algorithms or improve ones that already exist. This concept can be applied to both single- and multi-objective optimization strategies, which encourages continuous advancement in the area. This concept is particularly relevant in smart buildings, where traditional optimization methods struggle to balance the complex relationship between comfort indices (including temperature, illuminance, and air quality) and energy consumption patterns.

Multi-objective optimization algorithm design involves tackling two key challenges: guaranteeing solutions that are evenly spaced along the front and reaching convergence to the actual Pareto front. Significant advancements have been made in multi-objective optimization, leading to the creation of various algorithms designed to tackle the complexities of solving problems with multiple objectives. NSGA [33] stands as one of the most prominent and successful variations of Genetic Algorithms, widely adopted for multi-objective optimization problems. Other well-established techniques in this field include Multi-Objective Ant Colony Optimization (MOACO) [34], Multi-Objective Differential Evolution (MODE) [35,36], Multi-Objective Grasshopper Optimization Algorithm (MOGOA) [37,38], and Multi-Objective Particle Swarm Optimization (MOPSO) [39,40], among many others. These algorithms have proven effective in identifying non dominated solutions and approximating the Pareto front across a range of optimization problems. However, real-world applications often demand tailored approaches to address specific objectives and problem structures effectively.

Expanding on this knowledge, A novel Multi-Objective Evolutionary Mating Algorithm (MOEMA) is presented in this study, which draws inspiration from the EMA foundation [41] designed to address existing gaps in multi-objective optimization techniques, with specific application to smart building systems. MOEMA sets itself apart with two primary strategies: first, it employs an enhanced crowding distance function inspired by the NSGA to achieve more refined solution differentiation. Second, it implements the integration of Levy flight mechanics for enhanced exploration capabilities. To enhance its performance and exploration capabilities, MOEMA, a more sophisticated algorithm designed with non-dominated sorting, Levy flights, and an archive update mechanism in mind for multi-objective optimization problems. Whereas EMA uses a single-objective optimization technique to find a single optimal solution that maximises the weighted sum of user comfort and energy consumption, MOEMA uses a multi-objective optimization technique to find a set of Pareto optimal solutions that balance the two competing objectives [16]. EMA approaches prove impractical for the complex trade-offs between comfort index and energy efficiency.

Levy flight mechanics, characterized by random walks with step lengths following a power-law distribution, have been incorporated into optimization algorithms to enhance exploration capabilities [29,42]. This stochastic process allows algorithms to perform both local and long-distance searches, thereby avoiding local optima and improving the likelihood of discovering globally optimal solutions [43]. Integrating Levy flights into MOEMA offers a promising avenue for enhancing their ability to traverse rugged fitness landscapes and maintain diversity, which is particularly beneficial for applications requiring a delicate balance between multiple conflicting objectives, such as in smart building systems [44]. Levy flight was chosen for its ability to balance local and global search through power-law step distribution, making it ideal for smart building optimization with competing comfort and energy objectives. Its stochastic nature helps MOEMA escape local optima and explore diverse solution regions, effectively handling the nonlinear

relationships between occupant comfort and energy efficiency.

Zitzler-Deb-Thiele (ZDT) benchmark functions [45] have emerged as the gold standard for evaluation, and rigorous methodologies are necessary for the validation of multi-objective optimization algorithms. These functions offer a methodical framework for evaluating an algorithm's ability to find and approximate Pareto-optimal solutions. Numerous algorithms have attempted to solve these benchmark problems, such as Multi-Objective Flower Pollination Algorithm (MOFPA), MOALO, MOPSO, NSGA-II, and many more [46–51]. In smart building optimization, challenges include managing nonlinear relationships and balancing comfort with energy efficiency. ZDT functions serve as valuable benchmarks because they simulate real-world conditions through varied Pareto front shapes and complex interactions like building dynamics. Testing optimization algorithms like MOEMA on these functions helps validate their effectiveness before deploying them in actual smart building applications.

The application of MOEMA to smart building systems addresses a critical need in modern infrastructure management. Most of the energy used worldwide is consumed by buildings, optimizing their operations while maintaining the comfort index represents a crucial challenge in sustainable development. Building systems represent a critical application area for multi-objective optimization, where the optimization of comfort index and energy consumption often presents conflicting objectives. Comfort index metrics, including temperature, illumination, and air quality, require precise regulation to ensure a conducive indoor environment [52]. Simultaneously, minimizing energy usage is imperative for sustainability and cost reduction. Traditional optimization methods, such as linear programming and single-objective evolutionary algorithms, often fall short in effectively balancing these objectives because they are unable to depict the intricate interdependencies and dynamic nature of smart building environments [53].

The primary limitations of existing EMA and NSGA-II in the context of smart building optimization lie in their handling of multi-objective trade-offs. Traditional EMAs focus on single-objective optimization, relying on a weighted sum approach to combine multiple objectives into a single function. This method proves impractical for balancing conflicting objectives, such as comfort index and energy efficiency, as it often leads to suboptimal solutions that favor one objective over the other. On the other hand, while NSGA-II is a well-established multi-objective optimization algorithm, its crowding distance mechanism can struggle to maintain solution diversity in highly complex search spaces. This limitation can result in premature convergence, restricting its ability to explore the solution space effectively and find an optimal balance between comfort and energy consumption. To address these challenges, MOEMA introduces two key innovations: an enhanced crowding distance function inspired by NSGA, which improves solution differentiation and ensures better distribution of Pareto-optimal solutions, and the integration of Levy flight mechanics, which enhances exploration capabilities, prevents premature convergence, and enables a more thorough search of the solution space. By explicitly overcoming these gaps, MOEMA provides a more robust multi-objective optimization framework for smart buildings, achieving a more effective trade-off between user comfort and energy efficiency.

By rigorously testing MOEMA against established ZDT benchmark functions and applying it to real-world building scenarios, the purpose of this study is to show how well the algorithm finds the best trade-offs between comfort index and energy consumption. Furthermore, the study aligns with broader national objectives in artificial intelligence and Industry Revolution 4.0, highlighting its significance beyond purely theoretical contributions to practical applications in sustainable building management.

The following summarises the contributions made by this paper:

- a) Development of the Multi-Objective Evolutionary Mating Algorithm (MOEMA): MOEMA introduces a novel approach to multi-objective optimization, specifically designed to enhance comfort and energy

efficiency in smart buildings. It addresses the limitations of traditional methods by improving both convergence and solution diversity.

- b) Algorithmic Enhancements for Improved Optimization: MOEMA integrates an improved crowding distance function for better solution differentiation. It incorporates Levy flight mechanics to enhance exploration, balancing local and global search capabilities for superior performance.
- c) Validation and Application to Smart Buildings: MOEMA is evaluated against ZDT benchmark functions, demonstrating its effectiveness in solving multi-objective problems. It is applied to smart building systems, optimizing comfort metrics (temperature, illuminance, air quality) while reducing energy consumption, achieving superior performance compared to NSGA-II.

2. Multi-objective Evolutionary Mating Algorithm

The Multi-Objective Evolutionary Mating Algorithm (MOEMA) is an enhancement of the EMA created to solve multi-objective optimization issues. EMA is a metaheuristic algorithm that draws inspiration from organisms or the mating process [41]. The method is developed using the Hardy-Weinberg (HW) concepts, which are discussed in [54]. EMA begins with an initialization phase, similar to many other metaheuristic algorithms. Next, a selection phase takes place, followed by the reproduction of new offspring.

MOEMA enhances the original EMA framework through two key innovations: an improved crowding distance function inspired by the NSGA, and the integration of Levy flight mechanics for enhanced exploration capabilities. The research will develop a process for finding approximations near the actual Pareto optimal solutions. A key component of this method is the implementation of an improved crowding distance approach, inspired by NSGA. This enhanced crowding distance will be embedded into the EMA framework to better solve Pareto optimal problems. The method aims to improve upon the initial definition of crowding distance, addressing its limitations in distinguishing between solutions with similar crowding distances but different qualities. To improve the algorithm's capacity for exploration, the research will incorporate Levy flight randomization into the MOEMA framework. Step lengths in Levy flights, a kind of random walk, follow a heavy-tailed probability distribution. The algorithm should be able to explore the solution space more effectively with this method, which could result in the finding of better optimal solutions. The integration of Levy flights will replace the simple random number generation used in the original EMA, with the goal of preventing early convergence to local optima and broadening the range of possible solutions.

Levy flight was selected due to its ability to balance local and global search efficiency, which is crucial in optimizing smart building environments where multiple conflicting objectives (comfort index and energy consumption) exist. Unlike traditional random walk or Gaussian-based search strategies, Levy flight introduces a power-law step distribution that allows for both short-distance exploitation and long-distance exploration. This property is particularly beneficial in complex multi-objective optimization problems, such as smart building systems, where solutions often exist in diverse regions of the search space.

Furthermore, Levy flight's stochastic nature helps MOEMA escape local optima, ensuring broader exploration of the Pareto front and improving convergence to optimal trade-offs. This characteristic makes it particularly suitable for handling the dynamic and nonlinear nature of smart building environments, where achieving a fine balance between occupant comfort and energy efficiency requires adaptive search behaviour.

To clearly highlight the improvements introduced by the proposed MOEMA over the traditional EMA, a summarized comparison is presented in Table 1. While EMA is primarily designed for single-objective optimization, MOEMA incorporates multi-objective optimization principles, enabling it to effectively balance the trade-off between comfort

Table 1
Summarized comparison EMA and MOEMA.

Feature	Traditional EMA	MOEMA (Proposed)
Optimization Type	Single-objective optimization	Multi-objective optimization
Handling of Objectives	Uses a weighted sum approach, leading to potential bias towards one objective	Uses Pareto-based optimization to balance comfort index and energy consumption
Solution Diversity	Limited diversity due to reliance on weighted functions	Enhanced diversity using an improved crowding distance function
Exploration Mechanism	Basic evolutionary mating process	Integration of Levy flight for better global search
Selection Strategy	Best solution chosen based on fitness	Non-dominated sorting with archive update
Performance in Smart Buildings	Less adaptable to dynamic comfort-energy trade-offs	More effective in balancing comfort index and energy consumption

index and energy consumption in smart buildings. Additionally, MOEMA enhances solution diversity through an improved crowding distance function and strengthens its exploration capabilities by integrating Levy flight mechanics. Furthermore, unlike EMA, which relies on weighted sum approaches that may introduce bias, MOEMA employs Pareto-based optimization and a non-dominated sorting strategy to ensure a well-distributed set of optimal solutions. The key differences between the two algorithms are summarized in the table below.

A. Initialization

Like other evolutionary algorithms, MOEMA starts with an initialization procedure that creates a matrix-based population of search agents. The candidate of solution X included two groups for initialization: males, represented by X_m and women are identified by X_f , as defined in Eqs. (1) and (2). This ensures diversity and prepares the mating pools for subsequent iterations. This can be defined as follows:

$$X_m = \begin{bmatrix} x_1^1 & \dots & x_1^d \\ \vdots & \ddots & \vdots \\ x_{n/2}^1 & \dots & x_{n/2}^d \end{bmatrix} \quad (1)$$

$$X_f = \begin{bmatrix} x_{\frac{n}{2}+1}^1 & \dots & x_{\frac{n}{2}+1}^d \\ \vdots & \ddots & \vdots \\ x_n^1 & \dots & x_n^d \end{bmatrix} \quad (2)$$

In this case, the number of populations is n , and d is the dimension of the problem. Each population's objective or fitness function is assessed following the initialization procedure. After that, the best answer from each group is determined and stored.

B. Mating Process

The mating selection procedure is conducted at random. In this case, mating is assumed to occur based on the likelihood of adoption or the probability of sexual selection, I_{mates} which is represented as follows and discussed in Equations (3):

$$I_{mates} = I_{sex_ratio} + [*I_{mates(t)} - *I_{mates(k)}] \quad (3)$$

In this context, I_{sex_ratio} is assigned the value of 1 to indicate a balanced sex ratio with an equal count of males and females within the population. The variables $*I_{mates(t)}$ and $*I_{mates(k)}$ represent the weighted probabilities affecting sexual selection, attributed to variations in female availability across time (t) and space (k), respectively. The term I_{mates} encompasses the overall diversity in mating success, distinguished by various selective opportunities stemming from (i) fluctuations in the sex

ratio throughout the breeding period, (ii) the temporal and spatial accessibility of potential mates, and (iii) the general availability of mates, as referenced in [41]. This algorithm modifies these two factors to reflect the differential in fitness between males and females, thereby influencing the likelihood of sexual selection for each gender. Consequently, this adjustment has led to a revision in Eq. (3).

$$I_{mates} = 1 + \left[\text{var}(X_{m,*}^T) - \text{var}(X_{f,*}^T) \right] \quad (4)$$

Here, $\text{var}(X_{m,*}^T)$ and $\text{var}(X_{f,*}^T)$, denote the variance in selection for males and females, respectively, at iteration T . It should be noted that 't' and 'k' previously denoted the temporal and spatial variations in the availability of females, but these symbols have been removed to simplify the notation. In the updated version, refer to, $X_{m,*}$ and $X_{f,*}$ instead. According to Eqs. (1) and (2), $X_{m,*}$ and $X_{f,*}$ represent the selected individuals from the male and female groups, respectively, during the mating process. This selection is essential for producing new offspring in each iteration, wherein the value of I_{mates} can be positive or negative. When generating new offspring, the Hardy-Weinberg equilibrium is applied, and the new offspring X_{child}^T can be expressed as follows:

$$X_{child}^T = \begin{cases} p \cdot X_{m,*}^T + q \cdot X_{f,*}^T & \text{for } I_{mates} \geq 0 \\ p \cdot X_{f,*}^T + q \cdot X_{m,*}^T & \text{for } I_{mates} < 0 \end{cases} \quad (5)$$

where the normal random distribution, denoted by p , is written as follows:

$$p = \text{randn}(1, d) \quad (6)$$

In this context, q is defined as $(1-p)$. When the variance of $X_{f,*}^T$ is notably higher than that of $X_{m,*}^T$, as indicated by a negative value in Eq. (4), the characteristics of $X_{f,*}^T$ will predominantly influence the traits of the new offspring, governed by the probability p . It's worth noting that the terms p and q are connected to the Hardy-Weinberg principle, which has been previously explained. These values correspond to the genetic contributions from the mother and father, respectively. It is crucial to understand that, given the use of a normal distribution, the value of p could potentially be negative. Nevertheless, the Hardy-Weinberg equilibrium is still adhered to, maintaining the invariant that the sum of p and q is always 1.

This allows for both the increase and decrease of traits inherited from the mother or father, which can help the offspring generation solve optimization problems. Although a single mating can result in multiple offspring in nature, this algorithm assumes that each mating will result in one offspring. However, it may be substituted for both in that iteration process if the offspring's fitness is superior to that of the chosen mother and father.

Additionally, the current best solution that was saved during the initialisation process and at each iteration can also have an impact on the dimension of the offspring that are produced. Consequently, the new child is created in the manner described below:

$$X_{child}^T = K \cdot X_{child,j}^T + X_j^{best} \cdot (1-K), j = 1, 2, \dots, d \quad (7)$$

Here, X_j^{best} represents the optimal solution identified at a given iteration, and the value of K can be determined using the following formula:

$$K = \text{randn}(1, d) < C_r \quad (8)$$

where C_r is the crossover probability's predetermined value as it applies to DE. In this manner, the decision to swap out each dimension component with the optimal solution can be made at random. Eq. (7) will then be used to evaluate the offspring, calculating and comparing their objective function or fitness to that of their parents. The produced offspring is added to the parent pool if the offspring's fitness is higher. It is important to note that the offspring may replace the parents (either one or both) that lead the quick, ideal search process if it computes a

higher level of fitness.

C. Exploration process

In nature, environmental factors like food, source dispersion, predation, sociality, etc., have an unavoidable impact on the evolution of the mating system [41]. These environmental factors are modelled in the EMA to improve the algorithm's capacity for exploration, especially in the presence of predators.

An organism must choose whether to face or flee from the predator when it encounters them during the mating process. Whether the offspring is presumed to be alive or dead, this will drastically alter the best solution's characteristics. An organism is presumed to be alive if its fitness value has the potential to increase, and dead if it has a lower fitness value. The likelihood of running into the predator, r , in EMA must be adjusted in accordance with the optimization issues that must be resolved. The following rules govern how the exploration process is enforced at each iteration:

$$X_{child}^{T+1} = \text{rand}(1, d) \cdot X_j^{best} \text{ for } r < [0, 1] \quad (9)$$

The user sets the preset value, such as 0.2, that determines the likelihood of running into the predator. If the random number r is less than 0.2 at a given iteration, the Eq. (9) is enforced, causing exploration to take place. Apart from the population size and the maximum number of iterations, only two parameters— C_r and r —need to be adjusted based on the development.

In addition to this, Levy flight randomization further enhances exploration by generating large steps that can span distant regions of the solution space. The algorithm can break out of local optima and investigate new, possibly more promising regions thanks to Levy flight. A Levy distribution, which has the power-law formula $L(s) \sim |s|^{-(1-\beta)}$, where $0 < \beta \leq 2$ is an index, is used to determine the step length for Levy flight. Beginning at a single, well-known spot, the algorithm will produce an entirely new generation at randomly distributed distances based on Levy flights. The most promising member of the new generation will then be chosen after evaluation. Until the criteria for stopping are fulfilled, the procedure is repeated. Only the best option is selected. As a result, the equation for the new generation will be altered as follows:

$$X_{child}^T = X_j^{best} + \text{Levy}(N) \quad (10)$$

where the following formula is used to calculate Levy flight:

$$\text{Levy}(N) = 0.01 X \frac{r_1 X \sigma}{|r_2|^{\frac{1}{\beta}}} \quad (11)$$

Where σ is determined as follows, r_1 and r_2 are random numbers [0–1], and β is a constant in the value of 1.5.

$$\sigma = \left(\frac{\tau(1+\beta) \times \sin\left(\frac{\pi\beta}{2}\right)}{\tau\left(\frac{1+\beta}{2}\right) \times \beta \times 2 \left(\frac{\beta-1}{2}\right)} \right)^{\frac{1}{\beta}} \quad (12)$$

Levy flight randomization complements Eq. (9) by enabling long jumps, ensuring that the search spans both local and global regions of the solution space effectively. The fitness of the new offspring is assessed and contrasted with that of the parents after it is created using either Levy flight or Eq. (9). By replacing one or both parents if the offspring is more fit, exploration helps to expand the pool of potential solutions. The exploration phase in EMA strikes a balance between local diversification and global search by combining these mechanisms predator interactions, which are modelled by Eq. (9) and Levy flight randomization and greatly improving the algorithm's ability to find the best answers.

D. Archive and Crowding Distance

The archive in the MOEMA serves as a repository of non-dominated solutions, which, in terms of Pareto optimality, are the best options. During the algorithm's execution, new candidate solutions (offspring) are generated and evaluated. After that, the archive is updated by adding solutions that don't conflict with any already-existing solutions, ensuring that the algorithm retains only the most diverse and optimal solutions in terms of both objectives. This procedure aids in maintaining a collection of superior solutions that reflect a variety of trade-offs between the various goals. The archive's size is capped to maintain a manageable number of solutions and prevent the algorithm from becoming too computationally expensive. This size limit is typically enforced using crowding distance as a mechanism to prioritize solutions that are spread out across the objective space.

To maintain diversity among the solutions stored in the archive, crowding distance is used to measure the spacing between solutions within the objective space. This method ensures that the archive encompasses a representative coverage of the Pareto front by assigning preference to solutions that are more distant from one another in terms of their objective values. The crowding distance for a solution is obtained by sorting the population based on each objective and then measuring the distance between adjacent solutions in the sorted list. The crowding distance, denoted as d_i , for a specific solution i , is computed in the following manner:

$$d_i = \sum_{m=1}^M \left(\frac{f_{i,m+1} - f_{i,m-1}}{f_{max,m} - f_{min,m}} \right) \quad (13)$$

Since boundary solutions (those at the extremes of the population in each objective) are the most extreme in terms of objective values, the crowding distance gives them an infinite distance. Once the crowding distance for each solution has been calculated, the population is arranged in descending crowding distance order. This keeps the archive diverse by ensuring that solutions with greater crowding distances—those that are more dispersed—are kept. Only the most varied solutions—those with the greatest crowding distances—are retained if the archive grows beyond its maximum size. By using a crowding distance-based selection method, the archive is guaranteed to contain evenly distributed solutions across the Pareto front.

3. Problem formulation

This chapter presents the problem formulation used to assess the effectiveness of the suggested MOEMA. The formulation includes two critical aspects: testing on standard multi-objective benchmark functions and practical use in smart building systems to maximise user comfort and energy efficiency.

The proposed MOEMA algorithm will first be rigorously tested using the ZDT benchmark functions, which are frequently used to assess an algorithm's effectiveness, consistency, and capacity to approximate Pareto-optimal solutions in multi-objective optimization. These functions provide a starting point for evaluating MOEMA's ability to handle a variety of multi-objective problems with different features.

Following this, the application of MOEMA in a real-world scenario is introduced, concentrating on maximizing user comfort and energy use in a smart building setting. The aim is to achieve an optimal balance between user comfort and energy efficiency, considering environmental factors such as temperature, illumination, and indoor air quality. This dual-objective optimization problem not only demonstrates the practical significance of MOEMA but also highlights its effectiveness in addressing real-world challenges.

The problem formulation in this chapter provides a foundation for implementing and evaluating MOEMA, ensuring a systematic approach to validate its performance in both theoretical and practical contexts.

3.1. ZDT benchmark functions

The proposed MOEMA will be rigorously tested using ZDT benchmark. The performance of MOEMA is assessed and compared using the well-known ZDT benchmark functions (ZDT1 through ZDT6), which were first presented by Zitzler, Deb, and Thiele [45]. Two opposing objective functions, f_1 and f_2 , are used in the design of each ZDT function to produce a variety of Pareto front shapes, including convex, concave, and discontinuous fronts. In the context of smart buildings, optimization challenges involve nonlinearity, trade-offs between conflicting objectives (comfort index vs. energy efficiency), and the need to maintain solution diversity across a range of feasible settings. The ZDT functions capture these key aspects through diverse Pareto Front shapes, including convex, concave, and discontinuous Pareto fronts, which mimic the varying relationships between comfort parameters and energy consumption in real-world buildings. Some ZDT functions introduce deceptive properties, non-uniform search spaces, and variable interaction effects—like how external environmental factors and building dynamics impact optimization in smart buildings. By testing MOEMA on these benchmark functions before applying it to real-world smart building problems, we ensure that the algorithm effectively handles different types of multi-objective landscapes.

While ZDT functions do not capture all the complexities of real-world building environments, their mathematical diversity provides a controlled yet challenging evaluation framework. To further bridge this gap, we also validate MOEMA through real-world smart building simulations, demonstrating its applicability beyond theoretical benchmarks.

The objective functions of ZDT1, ZDT2, and ZDT3 are based on a straightforward linear or sinusoidal relationship, whereas ZDT4 adds multimodality, and ZDT6 poses problems with non-uniform distribution. Researchers can measure convergence efficiency, analyse solution diversity along the Pareto front, and evaluate algorithms' ability to reach a true Pareto-optimal set by using the ZDT functions, which provide known Pareto front shapes. These functions are fundamental to the study of multi-objective optimization because they aid in the evaluation and enhancement of algorithms, which enable their application to multi-objective problems in the real world. Table 2 below show the mathematical formulation for these ZDT's functions.

3.2. MOEMA for optimizing user comfort and energy consumption

The optimization process in this study is driven by a multi-objective cost function aimed at reducing energy use while increasing user

Table 2
Mathematical formulation for ZDT's.

Function	Mathematical formulation	D	Range
ZDT1	$F_1 = x_1, F_2 = g(1 - \sqrt{F_1/g}), g = 1 + \frac{9}{d-1} \sum_{i=2}^d x_i$	30	$x_i \in [0, 1]$
ZDT2	$F_1 = x_1, F_2 = g(1 - (F_1/g)), g = 1 + \frac{9}{d-1} \sum_{i=2}^d x_i$	30	$x_i \in [0, 1]$
ZDT3	$F_1 = x_1, F_2 = g(1 - \sqrt{F_1/g} - F_1/g \sin(10\pi F_1)), g = 1 + \frac{9}{d-1} \sum_{i=2}^d x_i$	30	$x_i \in [0, 1]$
ZDT4	$F_1 = x_1, F_2 = g(1 - \sqrt{F_1/g}), g = 1 + 10(d - 1) + \sum_{i=2}^d (x_i^2 - 10 \cos(4\pi x_i))$	10	$x_1 \in [0, 1]$ $x_i \in [-5, 5]$ $i = 1, \dots, D$
ZDT6	$F_1 = 1 - \exp(-4x_1) \sin^6(6\pi x_1), F_2 = g(1 - (F_1/g)^2), g = 1 + 9 \left(\frac{\sum_{i=2}^d x_i}{d-1} \right)^{0.25}$	30	$x_i \in [0, 1]$

comfort in a building environment. This function leverages data collected from [15], specifically temperature in Celsius, Illumination, and Indoor Air Quality readings. These data serve as reference points and scaling coefficients within the cost calculation, ensuring the optimization is grounded in real-world conditions rather than relying on abstract assumptions.

The cost function evaluates proposed control settings for each of the 48 time periods under consideration, determining both a comfort index based on deviations from desired temperature (22.78°C), illuminance (800 lux) and IAQ (800) and the associated energy consumption by measuring the absolute differences between the control settings and observed values. The objective is to find control settings, defined by a vector of temperature, lux and IAQ values for each time period, that balance the two conflicting objectives of maximizing user comfort (minimizing the negative of average comfort index) and minimizing energy consumption (minimizing average energy consumption).

In this way, the use of real-world data from the environment shapes the cost function and provides a context-specific optimization tailored to the reading behaviour of the environment under test, and penalizing control values that drastically deviate from the current environment conditions in terms of energy consumption.

In a smart building environment, the multi-objective cost function seeks to strike the best possible balance between energy use and user comfort. This cost function is intended to be used in a multi-objective optimization framework that aims to optimize these two conflicting objectives at the same time. Here is a detailed examination of each goal:

A. User Comfort (Objective 1)

The degree of comfort that building occupants experience is measured by the comfort index. It is typically influenced by factors such as temperature, illuminance levels, and indoor air quality. Each of these factors contributes to overall comfort, and deviations from desired setpoints can decrease comfort.

The comfort index (CI) for each period combines three components—temperature (T), LUX (L), and IAQ (I)—weighted equally with coefficients $p_1=1/3$, $p_2=1/3$, $p_3=1/3$. The comfort for each component is calculated based on the deviation of the decision variables from desired setpoints. The comfort index seeks to measure the level of comfort that the building's occupants experience. It considers three factors: First on how close the current temperature (T_k) is to a desired temperature (T_d). Second is how close the current illuminance level (L_k) is to a desired illuminance level (L_d). And third on how close the current IAQ level (I_k) is to a desired IAQ level (I_d). The desired value for each of the factor is as: desired temperature $T_d = 22.78$, desired Lux $L_d = 800$, desired IAQ $I_d = 800$. For each period k the comfort for each variable is expressed as:

$$T_i = 1 - \left(\frac{T_k - T_d}{T_c} \right)^2, L_i = 1 - \left(\frac{L_k - L_d}{L_c} \right)^2, I_i = 1 - \left(\frac{I_k - I_d}{I_c} \right)^2 \quad (14)$$

Here, T_c , L_c , and I_c are scaling coefficients for each variable, representing acceptable ranges that appears to be time varying. These coefficients likely represent the sensitivity or range of acceptable values for each factor at a given time. The comfort index scaling coefficients (T_c , L_c , I_c) are dynamically extracted from the dataset for each of the 48 time periods, allowing the comfort model to adapt to real-world conditions instead of using static values [15]. This approach accounts for variations in occupant preferences, external climate conditions, and building operational constraints. For instance, a higher T_c value during certain periods might indicate lower temperature sensitivity due to adaptive occupant behavior or external heat gain.

By incorporating time-dependent coefficients, the model ensures a more robust comfort-energy trade-off across diverse operating conditions. Future improvements could involve real-time learning mechanisms to further refine these coefficients using sensor feedback, making

the optimization framework more responsive to environmental dynamics and occupant needs. The comfort index $CI(k)$ for period k is then:

$$CI(k) = p_1 \cdot T_i + p_2 \cdot L_i + p_3 \cdot I_i \quad (15)$$

The individual components are combined using weights (p_1 , p_2 , p_3), which determine the relative importance of temperature, illumination, and IAQ to overall comfort. In the study, these are all set to 1/3, indicating equal importance.

The score ranges from 0 (least comfortable) to 1 (most comfortable). The overall comfort objective is the average of the CI values across all periods, CI_{avg} .

B. Energy Consumption (Objective 2)

The energy consumption component estimates how much energy is used to maintain the desired comfort levels. It's calculated based on the difference between the current settings (T_k , L_k , I_k) and the coefficients ($T_c(k)$, $L_c(k)$, $I_c(k)$), which might represent ambient or initial conditions.

The energy consumption (EC) for each period k is computed as the weighted sum of absolute deviations of each variable from their baseline coefficients, using weights $p_T=9$ for temperature, $p_L=9$, and $p_I=1$ for IAQ. This weight reflects the significant energy demands of temperature regulation compared to illuminance and indoor air quality systems. Heating and cooling systems (HVAC) are typically the most energy-intensive components in a building, consuming substantially more power than illuminance or air quality management systems. By assigning a much higher weight to temperature (9) relative to illuminance (1) and IAQ (1), the optimization algorithm acknowledges the disproportionate energy cost of thermal management.

This weighting approach ensures that the multi-objective optimization algorithm is particularly cautious about temperature modifications. Small changes in temperature require extensive energy input from heating or cooling systems, whereas adjusting illuminance levels or air quality can be achieved with minimal energy expenditure. The 9:1:1 ratio effectively communicates that a degree of temperature change is nine times more energetically significant than an equivalent change in illuminance or indoor air quality. Consequently, the algorithm will prioritize energy efficiency by minimizing unnecessary temperature fluctuations, while allowing more flexibility in illuminance and air quality adjustments.

The practical implication of these weights is a more nuanced and energy-conscious approach to building climate control. Instead of making frequent, small temperature changes that would consume considerable energy, the optimization strategy will seek solutions that maintain thermal comfort with minimal energy overhead. This approach aligns with modern sustainable building design principles, where energy efficiency is a critical consideration alongside occupant comfort.

Each component's energy use is proportional to the absolute difference between the current setting and the coefficient, scaled by a weight (p_T , p_L , p_I). The absolute difference is used because energy is consumed whether you are heating or cooling, increasing or decreasing illuminance, etc.

$$ET = p_T \cdot |T_k - T_c|, EL = p_L \cdot |L_k - L_c|, EI = p_I \cdot |I_k - I_c| \quad (16)$$

The total energy consumption $EC(k)$ for each period is:

$$EC(k) = ET + EL + EI \quad (17)$$

The total energy consumption for that time period is calculated by adding the energy consumption for temperature, illumination, and IAQ. The average energy consumption across all periods, EC_{avg} , represents the energy consumption objective. The energy consumption values for all 48 periods are averaged to get a single measure of average energy consumption.

C. Objective Formulation

In multi-objective optimization, the function returns a vector with two objectives that are Maximizing Comfort: This is represented as minimizing the negative of the average comfort index: $-CI_{avg}$ and Minimizing Energy Consumption: This is represented directly as minimizing EC_{avg} . Thus, the objectives vector is given by:

$$objectives = [-CI_{avg}, EC_{avg}] \tag{18}$$

This dual-objective setup enables a Pareto optimization process, allowing the algorithm to find trade-offs between reducing energy use and increasing comfort.

The process flowchart is displayed in Fig. 1. This flowchart illustrates the workflow of the MOEMA, created to maximise energy use and user comfort in smart building systems. The process begins with loading the dataset, followed by parameter initialization and defining a multi-objective fitness function. The algorithm iterates through multiple runs, initializing the population, evaluating the initial population against the objectives, and maintaining an archive using non-dominated sorting and crowding distance.

Each iteration involves generating offspring through the mating process, exploring with Levy flights for diversity, and updating the archive. After all iterations and runs, the algorithm evaluates the best run based on spacing and diversity of solutions. It then plots the Pareto front, identifies the most balanced point, and displays results, including user comfort and energy consumption at the selected point. Finally, the temperature, lux, and IAQ are analysed post-optimization, then a comparative analysis concluding the process. This structured flow ensures a comprehensive approach to solving multi-objective optimization challenges in smart building systems.

4. Results and discussion

This section gives a detailed description of the experimental setup, shows the results, and discusses the findings in detail.

4.1. Experiment setup

Simulations for this study were conducted using MATLAB on a Windows 11 platform. To ensure an equitable comparison, Table 3 outlines the configuration of parameters for both the MOEMA and NSGA-II, where the NSGA-II information in [55] were used in this comparison. Both algorithms were set up with a population size of 50 and a maximum of 500 iterations.

The study assessed the best, average, median, worst, and standard deviation metrics for Generational Distance (GD), Inverted Generational Distance (IGD), and spacing to analyse and contrast the effectiveness of MOEMA and NSGA-II. To confirm each algorithm’s robustness, these metrics were computed for the ZDT benchmark functions. The GD, IGD and spacing were used because they allow us to comprehensively evaluate MOEMA’s performance in terms of convergence, diversity, and uniformity relative to a known true Pareto front. These metrics ensure that the algorithm can effectively handle theoretical multi-objective optimization challenges before being applied to real-world scenarios.

For the real-world test function in building scenario aimed at maximizing comfort index and energy savings, the study focused solely on the

Table 3
Parameter setting for MOEMA and NSGA-II.

Algorithm	Parameter setting
Both algorithms	Simulation runs = 20, maximum iteration = 500, Population size = 50,
MOEMA	Best Environment Impact Rate, $Cr = 0.1$ (probability for each dimension), Exploration Rate, $r = 0.2$ (uses archive’s solutions and Levy flights with a 0.20 probability) Levy flights, $\beta = 1.5$
NSGA-II	Crossover Probability = 0.9, Distribution Index ($\eta_{c,c}$) = 20

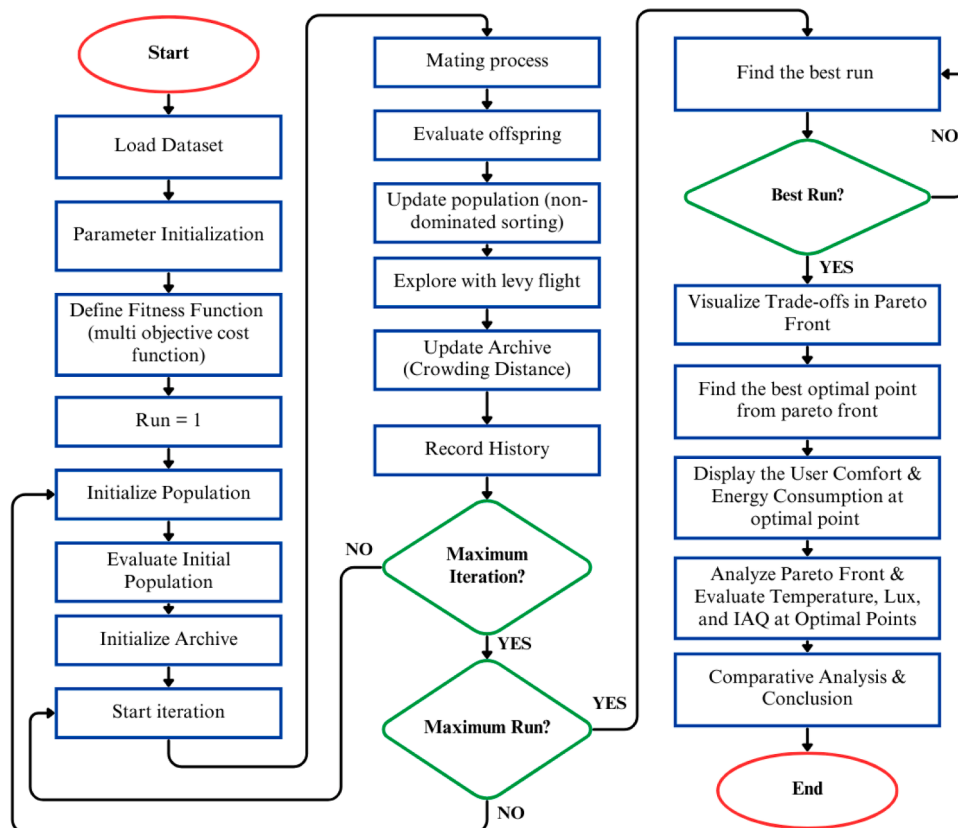


Fig. 1. MOEMA flowchart.

Spacing metric. This is because a true Pareto front is typically unavailable in practical applications, limiting direct comparisons on metrics like GD and IGD. Thus, Spacing serves as an essential indicator of solution distribution quality in these scenarios. For this implementation, spacing metrics were chosen because it is more sensitive to the quality of local distribution, ensuring that solutions remain well-distributed, it complements the crowding distance-based archive update mechanism, further improving diversity maintenance, it is more stable across different Pareto front shapes, making it suitable for the irregular and dynamic nature of real-world smart building optimization, it is less sensitive to the scale of objective functions, which is important when optimizing diverse comfort parameters and energy efficiency and it provides a good balance between uniformity and diversity, ensuring a well-spread set of optimization trade-offs for practical decision-making. Compared it to other metric like spread metrics, while both Spacing and Spread measure solution diversity, Spacing is more suitable for our smart building application because it's more sensitive to local distributions of comfort-energy trade-offs, remains consistent across various Pareto front shapes common in building dynamics, shows greater robustness to objective function scaling, and complements our algorithm's crowding distance mechanism. Unlike Spread, which focuses mainly on extreme points, Spacing provides better insight into intermediate solution distributions, ensuring more reliable diversity evaluation in smart building optimization where true Pareto fronts are typically unavailable.

To ensure the robustness of MOEMA, a sensitivity analysis was conducted to determine the optimal value for the Best Environment Impact Rate (Cr), Exploration Rate (r) and Levy flight parameter (β). For instance, the choice of $\beta = 1.5$ was based on prior research indicating that this value provides a balance between exploration and exploitation in optimization problems. To validate this setting, we conducted multiple simulation runs with different values of β (ranging from 1.1 to 2.0) and observed its impact on solution diversity and convergence. The results indicated that $\beta = 1.5$ provided the best trade-off between exploration and convergence speed, ensuring MOEMA's effectiveness in handling the comfort-energy trade-off in smart buildings. Additionally, other key parameters were fine-tuned to enhance MOEMA's performance. Best Environment Impact Rate ($Cr = 0.1$) and Exploration Rate ($r = 0.2$) were carefully selected based on multiple simulation runs to ensure optimal solution diversity. Once the best parameter settings were finalized, 20 independent simulation runs were conducted to validate the algorithm's consistency and determine the best trade-off between comfort index and energy consumption. These parameter settings were established to provide a fair comparison with NSGA-II while maximizing MOEMA's effectiveness in smart building optimization.

Assessment criteria for multi-objective optimization algorithms need to thoroughly examine both the solution quality and their spread across the Pareto front. For the evaluation of the MOEMA, three essential performance indicators are utilized. One of these metrics is the Generational Distance (GD), which gauges the precision of convergence by determining the mean Euclidean distance from the solutions on the identified Pareto front to their nearest points on the actual Pareto front, as cited in reference [56]. A smaller GD value signifies improved proximity to the true Pareto front. Generational Distance (GD) is calculated using the following equation:

$$GD = \left(\frac{1}{|P|} \sum_{i=1}^{|P|} d_i^p \right)^{\frac{1}{p}} \quad (19)$$

Moreover, the Inverted Generational Distance (IGD) employs the Manhattan distance to measure the average distance from each point on the actual Pareto front to its nearest counterpart on the obtained front, thereby evaluating both convergence and diversity [57]. IGD effectively assesses how well the obtained solutions cover the entire true Pareto front. Unlike GD, IGD flips the perspective and calculates distances from the true Pareto front to the obtained solutions:

$$IGD = \left(\frac{1}{|P^*|} \sum_{j=1}^{|P^*|} d_j^q \right)^{\frac{1}{q}} \quad (20)$$

The Spacing metric evaluates the evenness of the distribution of solutions along the resulting Pareto front by calculating the standard deviation of distances between consecutive solutions [56]. According to Schott, this metric quantifies the variability in distances between adjacent non-dominated solutions identified thus far [58]. A smaller Spacing value suggests a more consistent spread of solutions. The formula used to calculate the Spacing metric is as follows:

$$Spacing = \sqrt{\frac{1}{|P| - 1} \sum_{i=1}^{|P|} (d_i - \bar{d})^2} \quad (21)$$

4.2. ZDT benchmark function result

The performance analysis of the pareto front for MOEMA and NSGA-II using the ZDT benchmark functions is as figures below. These functions, which are widely used in multi-objective optimization, are made especially to evaluate the effectiveness, reliability, and precision of optimization algorithms when they approximate Pareto-optimal solutions.

By applying MOEMA and NSGA-II to the ZDT suite, which encompasses a diverse range of problem characteristics such as non-convex, discontinuous, and multimodal Pareto fronts, The purpose of this study is to thoroughly assess its capacity to resolve challenging multi-objective issues. The results obtained from these tests provide a foundational benchmark for comparing MOEMA's performance against other state-of-the-art optimization techniques.

Based on the analysis of all the figures, it appears that MOEMA and NSGA-II each demonstrate distinct strengths across different ZDT benchmark functions. These observations provide insights into their respective abilities to handle the diversity and convergence challenges presented by various kinds of optimization problems with multiple objectives.

For the ZDT1 function as in Fig. 2, which features a convex Pareto front, both MOEMA and NSGA-II achieve reasonably accurate representations of the true Pareto front. However, MOEMA distinguishes itself by producing a smoother and more continuous Pareto front. The distribution of solutions from MOEMA is notably uniform, ensuring a better spread across the front. NSGA-II, on the other hand, exhibits minor discontinuities and scattered points, which indicate some inconsistency in convergence or crowding-distance mechanisms. This suggests that MOEMA's selection and variation operators might be more effective at maintaining diversity and avoiding clustering of solutions. The uniformity achieved by MOEMA enhances its ability to approximate the true Pareto front comprehensively.

Regarding ZDT2, as shown in Fig. 3, both algorithms successfully capture the concave nature of the Pareto front. Both MOEMA and NSGA-II successfully converge to the true Pareto front, showcasing their ability to handle concave surfaces. Nevertheless, the smoothness and continuity of MOEMA's front are again superior. While NSGA-II performs adequately in capturing the overall concave shape, it exhibits minor irregularities in solution spacing, leading to some areas being denser than others. MOEMA's solutions, in contrast, are more uniformly distributed along the curve. This consistency highlights MOEMA's robustness in handling concave Pareto fronts and its ability to avoid solution crowding or gaps.

The ZDT3 benchmark function as in Fig. 4, which is known for its challenging disconnected Pareto front, provides a critical test of an algorithm's ability to preserve solution diversity across multiple segments. MOEMA demonstrates clear superiority here by accurately defining the disconnected segments with well-spaced solutions and distinct boundaries between regions. NSGA-II, while capable of identifying the

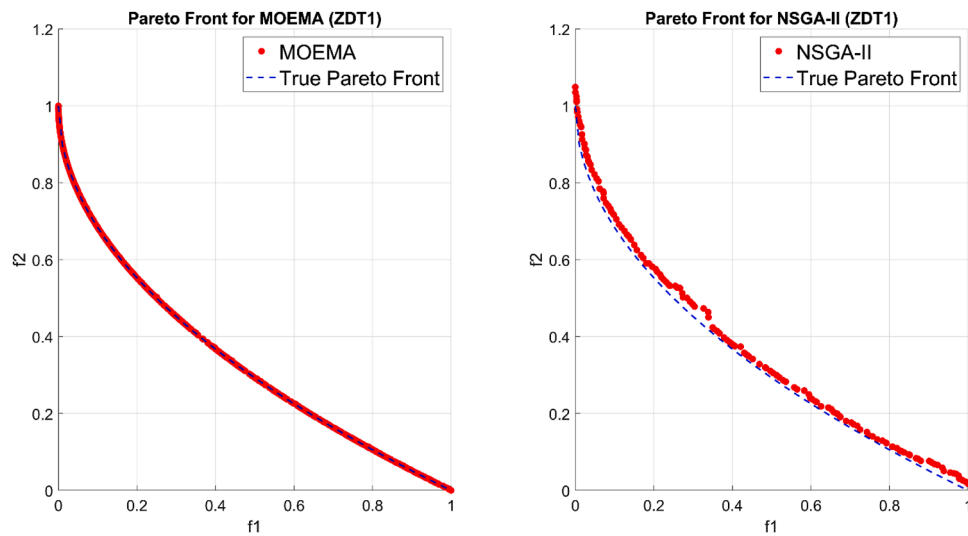


Fig. 2. Comparison pareto front MOEMA vs NSGA-II for ZDT1.

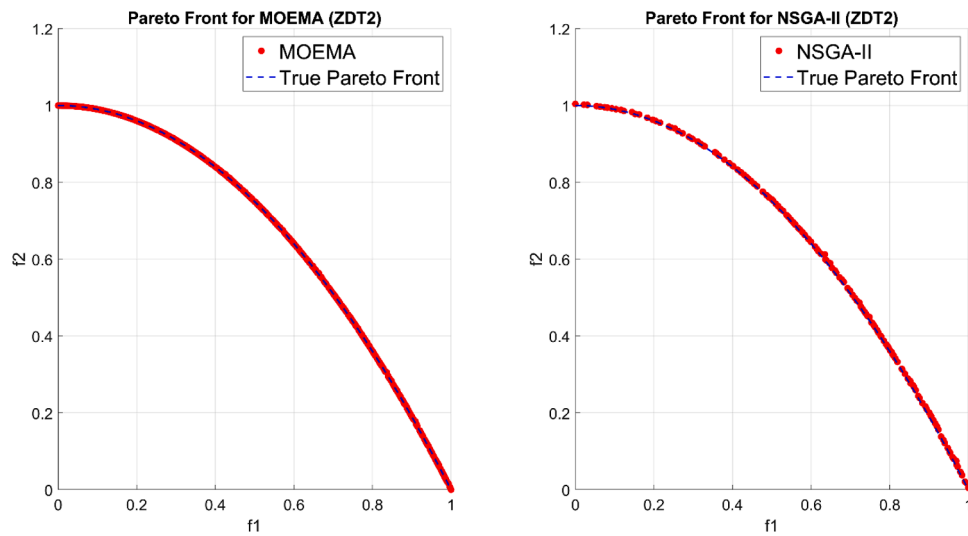


Fig. 3. Comparison pareto front MOEMA vs NSGA-II for ZDT2.

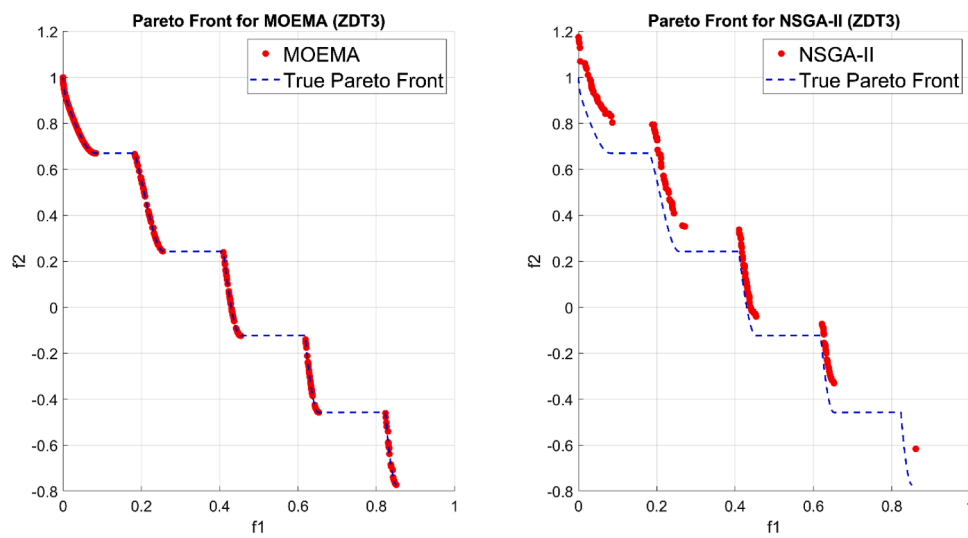


Fig. 4. Comparison pareto front MOEMA vs NSGA-II for ZDT3.

discontinuous nature of the front, produces more scattered solutions near the disconnection points. This scattering suggests potential challenges in maintaining stability during the search process, particularly near the edges of the disjointed regions. MOEMA's ability to maintain clarity in the disconnected areas underscores its robustness in preserving diversity and convergence simultaneously.

For ZDT4 as in Fig. 5, notorious for its numerous local Pareto fronts, presents one of the most difficult challenges for multi-objective optimization algorithms. Both MOEMA and NSGA-II demonstrate comparable performance in terms of convergence to the global Pareto front, effectively avoiding the traps of local fronts. However, MOEMA produces a smoother and more continuous Pareto curve, indicating better exploitation of the objective space. NSGA-II, while achieving similar convergence, displays slightly more scattered solutions, particularly in regions where the problem's ruggedness introduces additional difficulty. This scattered distribution suggests that NSGA-II may struggle with maintaining diversity under such challenging conditions, whereas MOEMA appears more resilient.

Finally, for ZDT6 as in Fig. 6, with its biased and non-uniform mapping of the search space, reveals marked differences in the algorithms' capabilities. MOEMA excels by producing a consistent and well-defined Pareto front, with solutions distributed uniformly across the objective space. This performance indicates that MOEMA effectively overcomes the search space bias and ensures comprehensive coverage of the front. NSGA-II, in contrast, struggles significantly with ZDT6, as evidenced by its scattered solutions and non-uniform distribution. The higher regions of the objective space, in particular, exhibit greater dispersion, suggesting that NSGA-II's diversity preservation mechanisms may falter in biased environments.

Overall, MOEMA demonstrates superior performance in terms of solution uniformity, continuity, and convergence across the test functions. Its ability to produce smooth and well-distributed Pareto fronts is particularly evident in the more challenging cases of ZDT3 and ZDT6. This suggests that MOEMA's design is inherently better suited to handle complex multi-objective landscapes, including those with discontinuities or non-uniform biases. NSGA-II, while competitive in simpler cases such as ZDT1 and ZDT2, shows signs of instability or reduced efficiency in problems with higher complexity.

These findings imply that MOEMA may be more robust and reliable for real-world multi-objective problems, particularly those requiring precise and uniform Pareto front approximations in challenging environments.

Three critical metrics—generational distance (GD), inverted generational distance (IGD), and spacing—were employed to evaluate and

compare the performance of MOEMA and NSGA-II, as presented in Table 4. For the ZDT1 problem, MOEMA exhibited significantly better results, achieving a GD average of 0.0083, far lower than NSGA-II's 0.0518, highlighting improved convergence towards the true Pareto front. This was further supported by MOEMA's lower IGD value (0.0027 vs. 0.0509) and superior spacing metric (0.0038 vs. 0.0052), indicating a more uniform solution distribution.

For ZDT2, MOEMA again demonstrated notable superiority, with a GD average of 0.0006 compared to 0.0093 for NSGA-II. Similar trends were observed in IGD (0.0029 vs. 0.0110) and spacing (0.0042 vs. 0.0047), underscoring MOEMA's higher solution quality and distribution uniformity. Additionally, MOEMA's lower standard deviations across all metrics reflected its consistent and reliable performance.

In tackling the ZDT3 problem, characterized by a discontinuous Pareto front, MOEMA maintained its advantage, achieving much better GD (0.0031 vs. 0.0739), IGD (0.0042 vs. 0.1464), and spacing (0.0048 vs. 0.0086) values. Furthermore, the markedly lower standard deviation for MOEMA (e.g., GD: 0.0001 vs. 0.0422) signified more stable and consistent results. For the ZDT4 problem, known for its numerous local Pareto fronts, MOEMA demonstrated exceptional performance, particularly in GD (0.0084 vs. 0.5892) and IGD (0.0027 vs. 0.5467). While the spacing metrics were closer (0.0030 vs. 0.0060), MOEMA still maintained an edge. The large disparity in standard deviations highlighted MOEMA's robustness in handling multimodal optimization challenges.

Finally, in the ZDT6 problem, characterized by non-uniform mapping, MOEMA showcased its most pronounced advantage. The GD (0.0184 vs. 1.2658) and IGD (0.0023 vs. 1.0450) values clearly indicated MOEMA's superior convergence and diversity. Additionally, the spacing metrics (0.0041 vs. 0.0174) reaffirmed MOEMA's ability to achieve better solution distribution. Overall, MOEMA consistently outperformed NSGA-II across all test cases, achieving superior best, average, median, and worst values while maintaining lower standard deviations, which emphasized its robustness and reliability. This comprehensive performance analysis highlights MOEMA as a more effective algorithm for solving multi-objective optimization problems, particularly in terms of stability, convergence precision, and solution diversity.

4.3. Optimizing energy consumption and user comfort in smart building systems problem result

Subsequently, the application of MOEMA in a real-world scenario is discussed, focusing on enhancing user comfort while reducing energy usage in a building. The problem considers various environmental

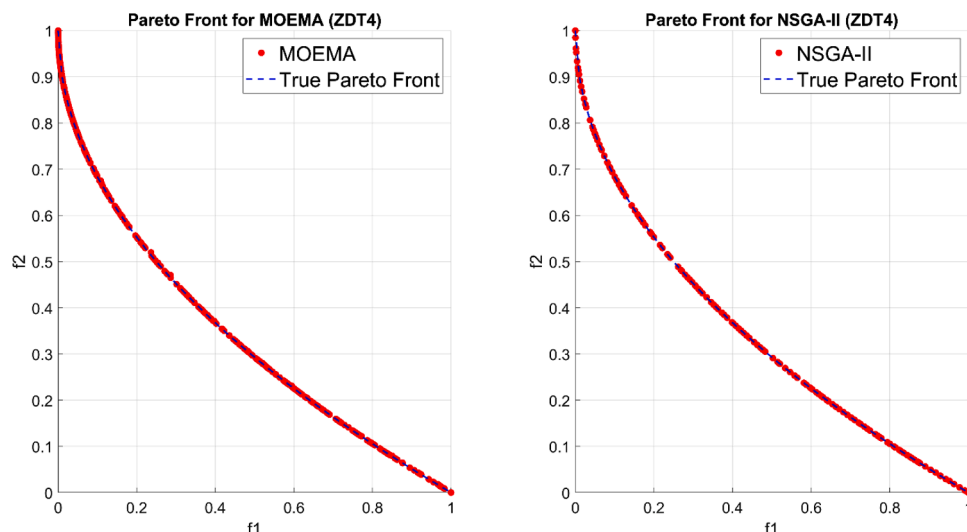


Fig. 5. Comparison pareto front MOEMA vs NSGA-II for ZDT4.

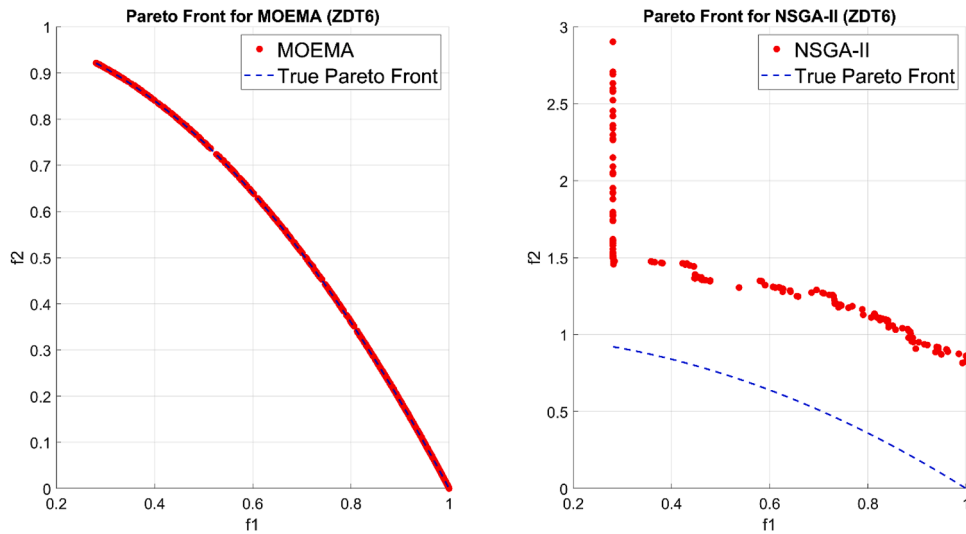


Fig. 6. Comparison pareto front MOEMA vs NSGA-II for ZDT6.

Table 4
Performance results of MOEMA vs NSGA-II for ZDTs benchmark functions.

Evaluation metrics		ZDT1		ZDT2		ZDT3		ZDT4		ZDT6	
		MOEMA	NSGA-II								
GD	Best	0.0077	0.0146	0.0005	0.0031	0.0029	0.0137	0.0078	0.0078	0.0042	0.7708
	Ave	0.0083	0.0518	0.0006	0.0093	0.0031	0.0739	0.0084	0.5892	0.0184	1.2658
	Median	0.0083	0.0493	0.0006	0.0094	0.0031	0.0668	0.0084	0.5637	0.0046	1.2300
	Worst	0.0091	0.1092	0.0007	0.0162	0.0034	0.1511	0.0091	1.2219	0.2818	1.7399
	Std Dev	0.0004	0.0265	0.0001	0.0044	0.0001	0.0422	0.0003	0.2909	0.0620	0.3136
IGD	Best	0.0024	0.0131	0.0027	0.0049	0.0035	0.0769	0.0023	0.0038	0.0019	0.7350
	Ave	0.0027	0.0509	0.0029	0.0110	0.0042	0.1464	0.0027	0.5467	0.0023	1.0450
	Median	0.0027	0.0489	0.0029	0.0106	0.0040	0.1511	0.0026	0.5261	0.0022	1.0204
	Worst	0.0030	0.1046	0.0030	0.0189	0.0059	0.2110	0.0030	1.1142	0.0026	1.5628
	Std Dev	0.0002	0.0255	0.0001	0.0050	0.0006	0.0458	0.0002	0.2654	0.0002	0.2485
Spacing	Best	0.0033	0.0043	0.0036	0.0041	0.0045	0.0034	0.0027	0.0054	0.0036	0.0092
	Ave	0.0038	0.0052	0.0042	0.0047	0.0048	0.0086	0.0030	0.0060	0.0041	0.0174
	Median	0.0039	0.0053	0.0042	0.0042	0.0048	0.0050	0.0030	0.0060	0.0041	0.0143
	Worst	0.0042	0.0060	0.0046	0.0068	0.0058	0.0401	0.0033	0.0066	0.0045	0.0408
	Std Dev	0.0002	0.0006	0.0003	0.0008	0.0003	0.0111	0.0002	0.0004	0.0002	0.0098

factors such as temperature, illumination levels measured in lux, and indoor air quality (IAQ) to achieve the optimal trade-off between user comfort and energy efficiency. This dual-objective optimization

challenge highlights not only the practical application of MOEMA in addressing complex issues but also demonstrates its efficacy in actual implementation.

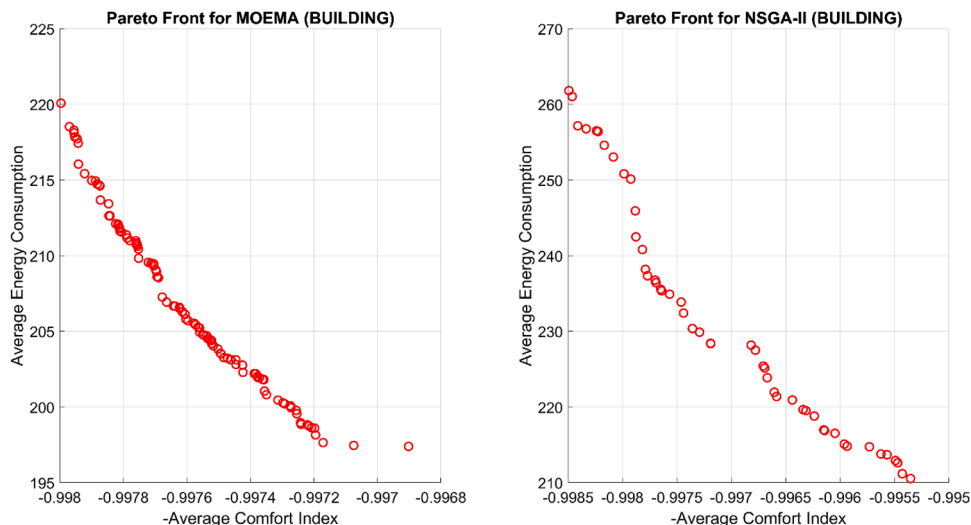


Fig. 7. Comparison pareto front MOEMA vs NSGA-II for building problem.

The main goals of this issue are to improve user comfort and reduce energy usage. Below is an analysis comparing the Pareto fronts produced by MOEMA and NSGA-II in the context of smart building systems. The test was run 20 times ensures a robust, unbiased, and statistically reliable evaluation, allowing for meaningful comparisons between MOEMA and NSGA-II. Then the best spacing pareto front are selected for comparison. The spacing metric is a valid strategy for selecting the best Pareto front because it measures the distribution and uniformity of solutions.

Spacing metrics were used for this implementation because it's more sensitive to local distribution quality, works well with the current archive update mechanism that uses crowding distance, more stable for problems with varying front shapes, less sensitive to the scale of objective functions and provides a good balance between diversity and uniformity.

Fig. 7 compares the Pareto fronts of the MOEMA and NSGA-II algorithms for building optimization, highlighting their distinct performance characteristics. The MOEMA algorithm demonstrates a more densely populated and uniform Pareto front, with solutions ranging from approximately -0.998 to -0.996 on the x-axis (negative comfort index) and 195 to 220 on the y-axis (energy consumption). In contrast, NSGA-II exhibits a slightly wider spread but less uniform distribution of solutions, spanning from about -0.998 to -0.995 on the comfort index axis and 210 to 260 on the energy consumption axis. The MOEMA's Pareto front shows superior convergence characteristics, evidenced by its lower energy consumption values for similar comfort levels, with its solutions consistently achieving energy consumption values below 220 units compared to NSGA-II's higher range extending up to 260 units.

The multi-objective cost function, which balances user comfort and energy consumption, reveals that MOEMA achieves more efficient trade-offs between these competing objectives. This is particularly evident in the lower region of the Pareto front, where MOEMA maintains better energy efficiency while preserving comfort levels. The comfort index calculation, incorporating weighted components for temperature ($p_1=1/3$), lux ($p_2=1/3$), and IAQ ($p_3=1/3$), demonstrates that both algorithms successfully maintain high comfort standards (as indicated by values close to -1), but MOEMA achieves this with notably lower energy consumption. This superior performance can be attributed to MOEMA's more effective exploration of the solution space, particularly in regions where marginal improvements in comfort require significant energy investments.

From an implementation perspective, MOEMA appears to be the more suitable choice for smart building optimization. Its pareto not only indicates better overall performance in terms of the energy-comfort trade-off but also provides decision-makers with a more consistent and a widely dispersed collection of ideal solutions. The denser distribution of solutions in MOEMA's Pareto front also suggests greater reliability and stability in the optimization process, making it a more robust choice for practical applications in smart building management systems.

Table 5 shows the comparison between MOEMA and NSGA-II's spacing performance on smart building systems. The spacing metric evaluation reveals that MOEMA demonstrates significantly better solution distribution compared to NSGA-II across all statistical measures. MOEMA achieves a best spacing value of 0.0406, which is substantially lower than NSGA-II's best value of 0.2295. This indicates that MOEMA

produces more uniformly distributed solutions along its Pareto front. The average spacing value for MOEMA (0.0935) is approximately four times better than NSGA-II (0.3667), suggesting consistently superior distribution of solutions across multiple runs.

Looking at the median values, MOEMA maintains its advantage with 0.0804 compared to NSGA-II's 0.3568, reinforcing the algorithm's consistent performance in maintaining uniform spacing. The worst-case spacing scenario for MOEMA (0.1743) is still considerably better than NSGA-II's worst case (0.6200), indicating that even in suboptimal conditions, MOEMA maintains more reliable solution distribution. Furthermore, MOEMA's lower standard deviation (0.0368 vs 0.0835) demonstrates more stable and predictable spacing performance across different optimization runs, making it a more dependable option for real-world uses in optimization issues with buildings environment.

These spacing metrics strongly support the visual analysis of the Pareto fronts and confirm that MOEMA provides a more evenly distributed and reliable set of optimal solutions compared to NSGA-II in the context of smart building optimization. Any point on the Pareto front plot can be selected for analysis. Typically, the balance point on the Pareto front is chosen as a reference to evaluate the performance of the algorithm. The "balance point" or "knee point" on the Pareto front is often chosen as a reference because it represents a solution were improving one objective significantly worsens another. This point can be used as a standard to assess how well an optimization algorithm performs and is typically regarded as a good trade-off between the objectives.

Fig. 8 show the comparison the balance point for MOEMA and NSGA-II. Looking at the balance points, MOEMA shows a balance point at coordinates (-0.997604, 205.81), while NSGA-II's balance point is at (-0.997359, 230.351). The comparison reveals that MOEMA achieves a better trade-off between comfort and energy consumption. In terms of comfort index, both algorithms perform similarly with only a 0.03 % difference (MOEMA at -0.997604 vs NSGA-II at -0.997358). However, for energy consumption, MOEMA demonstrates significantly better efficiency, requiring 205.81 units compared to NSGA-II's 230.351 units - a reduction of 24.541 units or approximately 10.65 % lower energy consumption. This indicates that MOEMA finds a more efficient compromise between the two objectives, providing an optimal solution that maintains nearly identical user comfort while achieving over 10 % better energy efficiency at the critical balance point.

The observed 10.65 % reduction in energy consumption achieved by MOEMA has significant practical implications for real-world building optimization. In a typical commercial building setting, where energy consumption is a major operational cost, this improvement translates to substantial reductions in electricity usage while maintaining occupant comfort. For example, if a building using NSGA-II requires 230 energy units for optimal operation, switching to MOEMA reduces this requirement to approximately 205.81 units. This improvement directly leads to lower energy costs and decreased carbon emissions, contributing to sustainable and cost-effective building management. When applied across large-scale buildings such as office complexes, hotels, or university campuses, these savings accumulate, resulting in considerable financial and environmental benefits. Furthermore, the enhanced energy efficiency achieved by MOEMA supports compliance with energy regulations and sustainability certifications, making it a highly effective solution for smart building operations. By optimizing the trade-off between comfort and energy use, MOEMA provides a practical and scalable approach to improving building efficiency without compromising occupant well-being.

The selection of the balance point in Fig. 8 is based on identifying the optimal trade-off between user comfort and energy consumption. This balance is determined by normalizing both comfort and energy values and computing their Euclidean distance from the ideal scenario, which represents maximum comfort with minimal energy usage. The results indicate that MOEMA achieves a more efficient balance compared to NSGA-II, maintaining nearly identical comfort levels (-0.997604 vs.

Table 5
MOEMA and NSGA-II's spacing performance on building systems.

Evaluation metrics		BUILDING SYSTEMS	
		MOEMA	NSGA-II
Spacing	Best	0.0406	0.2295
	Ave	0.0935	0.3667
	Median	0.0804	0.3568
	Worst	0.1743	0.6200
	Std Dev	0.0368	0.0835

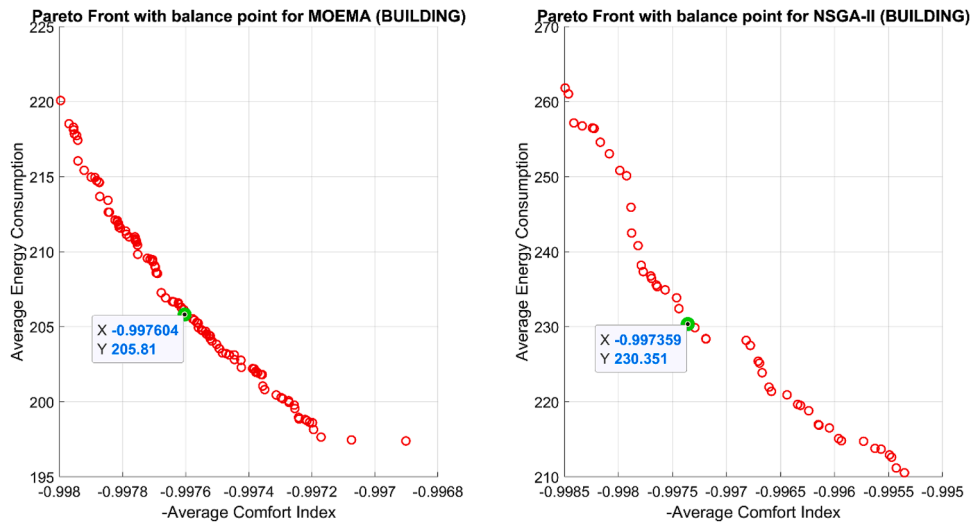


Fig. 8. Balance point for MOEMA vs NSGA-II for building problem.

-0.997359) while significantly reducing energy consumption by approximately 10.65 %. By deriving specific temperature, illuminance (lux), and indoor air quality (IAQ) settings from the balance point, the study provides practical guidelines for smart building management. These optimized parameters ensure a comfortable indoor environment while reducing energy costs and improving sustainability. The extracted settings can be dynamically adapted across different time periods, allowing for real-world implementation in energy-efficient building operations without compromising occupant well-being.

The balanced solution is defined as the point closest to the ideal scenario of maximum comfort and minimum energy use. By calculating the Euclidean distance from the normalized scale, the study derives a set of operational parameters that harmonize comfort and energy objectives. These optimized settings for temperature, lighting, and IAQ can be reshaped into a format applicable across different time periods, supporting sustainable building management by maintaining comfort while reducing energy consumption. These values are crucial design parameters from the optimization’s decision variables at those balance points. The comparison of MOEMA and NSGA-II algorithms at their respective balance points reveals distinct performance characteristics across all three control parameters.

Fig. 9 show the Temperature Before and After Optimization at

Balanced point. For temperature comparison, both algorithms demonstrate effective regulation around the desired setpoint of 22.78°C, with MOEMA exhibiting slightly more stable control with fewer fluctuations compared to NSGA-II. The temperature variations for MOEMA generally stay within a narrower band, suggesting more consistent thermal comfort for occupants. Moema achieves an average temperature of 22.713°C while NSGA-II achieves an average temperature of 22.518°C. This shows that Moema performs better than NSGA-II because Moema is closer to the desired value of 22.78°C, with only a 0.067°C difference.

Fig. 10 show the illuminance (Lux) before and after optimization at balanced point. In terms of illuminance, where the desired setpoint is 800 lux, both algorithms show dynamic responses to varying conditions. MOEMA demonstrates more aggressive adjustments to maintain optimal lux, as evidenced by its sharper transitions, while NSGA-II shows slightly smoother but less precise control. The MOEMA algorithm appears to track the setpoint more closely during peak demand periods, particularly noticeable in the time intervals between 25-35, where it maintains tighter control around the desired 800 lux level. MOEMA achieves an average Lux of 802.17 while NSGA-II achieves an average Lux of 793.16. This show that MOEMA is closer to desired value.

Fig. 11 show the IAQ before and after optimization at balanced point. For Indoor Air Quality (IAQ) control, both algorithms maintain values

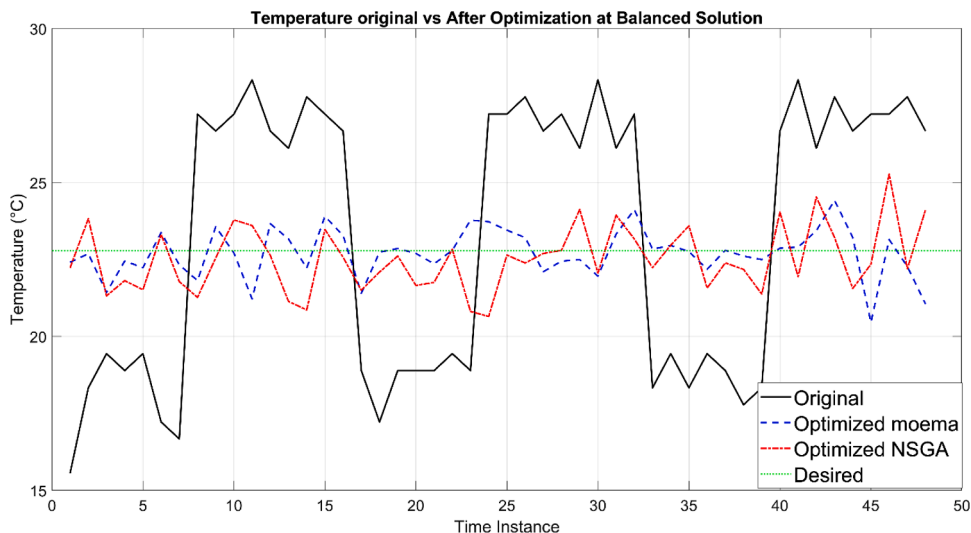


Fig. 9. Temperature before and after optimization at balanced point.

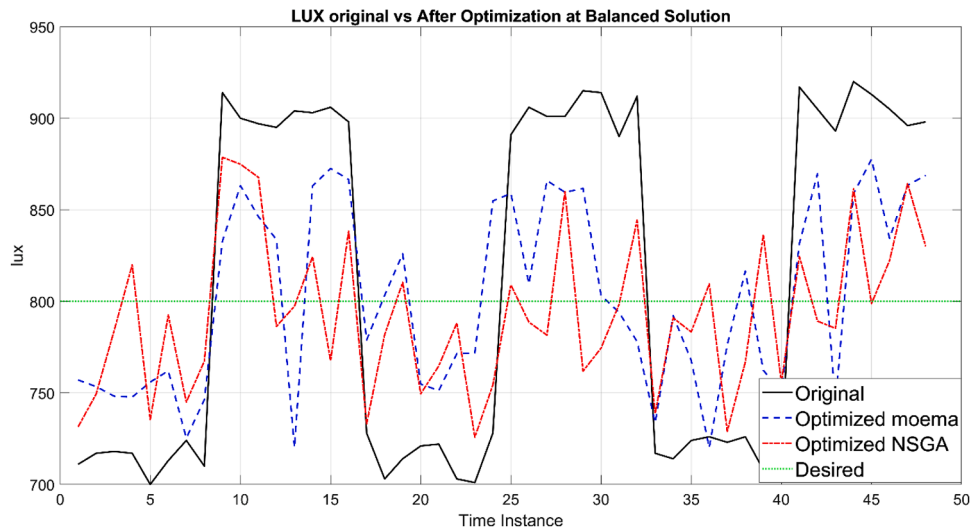


Fig. 10. LUX before and after optimization at balanced point.

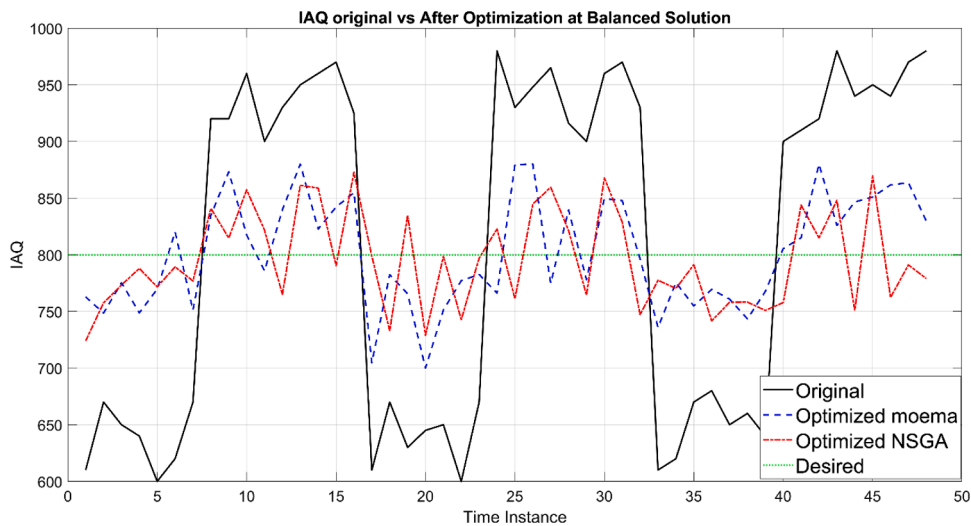


Fig. 11. IAQ before and after optimization at balanced solution.

near the desired setpoint of 800, but with distinct control strategies. MOEMA’s control pattern shows more responsive adjustments with shorter deviation periods from the setpoint, while NSGA-II exhibits a more conservative approach with gentler transitions but longer periods of slight deviation. The MOEMA algorithm demonstrates superior performance in rapidly returning to the setpoint after disturbances, particularly evident in the periods between 15–25 and 35–45 time intervals. The average IAQ for MOEMA is 801.84, whereas the average IAQ for NSGA-II is 795.43. Because MOEMA is closer to the target value of 800, this indicates that MOEMA outperforms NSGA-II. Overall, MOEMA’s more precise control across all three parameters contributes to its better energy efficiency while maintaining comparable comfort levels, as reflected in the earlier analysed balance point metrics. The comparison of temperature, Lux and IAQ at the balance point prove that the comfort index for MOEMA is slightly better than NSGA-II with only 0.03 % comfort difference as shown in the Fig. 8.

To validate the effectiveness of the proposed MOEMA against NSGA-II, the study conducted statistical significance tests on the optimization results for energy consumption and user comfort in smart building systems. Specifically, the study employed both the two-tailed *t*-test and the Wilcoxon rank test to compare the performance of the two algorithms across both objectives. The results, as shown in Table 6, indicate that

Table 6
statistical test for MOEMA vs NSGA-II.

Statistical test	<i>p</i> -value (two-tail)	Significant? ($\alpha = 0.05$)	Conclusion
<i>t</i> -test (objective 1)	4.9040E-06	Yes	Significant difference
<i>t</i> -test (objective 2)	2.7651E-15	Yes	Significant difference
Wilcoxon rank test (objective 1)	7.7000E-5	Yes	Significant difference
Wilcoxon rank test (objective 2)	0	Yes	Significant difference

MOEMA significantly outperforms NSGA-II in both objectives. For the *t*-test, the *p*-values obtained for objective 1 (comfort index) and objective 2 (energy consumption) were 4.9040E-06 and 2.7651E-15, respectively, both of which are well below the commonly accepted significance threshold of 0.05. This confirms that the observed performance differences are statistically significant. Similarly, the Wilcoxon rank test yielded *p*-values of 0.000077 and 0 for objectives 1 and 2, respectively, further reinforcing the conclusion that MOEMA provides a statistically significant improvement over NSGA-II. These results demonstrate that

MOEMA achieves superior optimization in balancing comfort and energy efficiency in smart buildings, highlighting its potential as an effective approach for real-world applications.

5. Conclusion

In conclusion, the proposed MOEMA has demonstrated significant advantages over NSGA-II in both theoretical benchmarks and practical smart building applications. Through extensive testing on ZDT benchmark functions, MOEMA consistently outperformed NSGA-II across all evaluation metrics, showing superior convergence, diversity, and stability as evidenced by better GD, IGD, and spacing values with notably smaller standard deviations. This theoretical superiority translated effectively to real-world applications in smart building optimization, where MOEMA achieved remarkable results in balancing comfort and energy efficiency. The algorithm's enhanced performance is particularly evident in its ability to maintain nearly identical comfort levels (-0.997604 vs -0.997359) while reducing energy consumption by 10.65 % compared to NSGA-II. This energy efficiency improvement has significant practical implications, as it directly translates to reduced operational costs and lower carbon emissions in real-world building management. By optimizing the trade-off between comfort and energy use, MOEMA enables more sustainable and cost-effective building operations, making it particularly valuable for commercial buildings, offices, and large-scale smart infrastructures.

MOEMA's superior control precision was further demonstrated in its management of specific environmental parameters, achieving closer adherence to desired setpoints for temperature (22.713°C vs 22.518°C), illumination (802.17 vs 793.16 lux), and indoor air quality (801.84 vs 795.43). These results validate that MOEMA's innovative integration of improved crowding distance function and Levy flight mechanics creates a more robust and efficient optimization framework for complex multi-objective problems, particularly in smart building systems where it successfully balances the competing demands of occupant comfort and energy efficiency. This advancement represents a significant contribution to both evolutionary computation and sustainable building management within the context of Industry 4.0.

Implementing MOEMA in real-world smart building optimization requires addressing computational complexity and scalability. The algorithm's computational demand scales with population size, iterations, and problem complexity, necessitating a balance between solution quality and efficiency. Potential improvements include parallel computing techniques like distributed processing and GPU acceleration, as well as hierarchical optimization strategies that optimize individual zones before aggregating building-wide solutions. Cloud-based deployment and edge computing integration could enable real-time optimization, allowing MOEMA to dynamically adapt to changing environmental conditions. Future research may explore adaptive population sizing and hybrid approaches with surrogate models to reduce computational overhead while maintaining solution accuracy, ensuring the algorithm's practicality for large-scale smart building applications.

Future research on MOEMA can explore both its applicability to diverse optimization scenarios and potential algorithmic enhancements. Beyond smart building management, MOEMA's adaptability makes it suitable for optimizing energy-efficient HVAC systems in smart grids, industrial process control, and transportation networks, where balancing multiple conflicting objectives is crucial. Furthermore, MOEMA can be extended to domains such as medical decision-making, supply chain logistics, and financial portfolio optimization, where effective trade-offs between risk, cost, and performance are essential. From an algorithmic perspective, MOEMA could benefit from adaptive parameter tuning, particularly for the Levy flight parameter β , to dynamically adjust exploration-exploitation trade-offs based on problem complexity. Hybrid approaches, such as integrating MOEMA with surrogate modelling or reinforcement learning techniques, could enhance its efficiency in high-dimensional and computationally expensive

problems. Additionally, refining its diversity preservation mechanisms, such as clustering-based improvements to crowding distance calculations, could further optimize Pareto front distribution and convergence behaviour. These advancements will expand MOEMA's versatility and effectiveness, making it a robust framework for solving complex multi-objective optimization problems across various domains.

CRedit authorship contribution statement

Muhammad Naim Bin Nordin: Writing – original draft, Visualization, Methodology, Data curation. **Mohd Herwan Sulaiman:** Writing – review & editing, Investigation, Conceptualization. **Nor Farizan Zakaria:** Resources, Project administration. **Zuriani Mustaffa:** Writing – review & editing, Validation.

Declaration of competing interest

The authors declare that they have no known competing financial interests or personal relationships that could have appeared to influence the work reported in this paper.

Acknowledgement

This work was supported by the Ministry of Higher Education Malaysia (MOHE) under the Fundamental Research Grant Scheme (FRGS/1/2024/ICT02/UMP/03/2).

Data availability declaration

Data sharing not applicable to this article as datasets can be obtained from the literature.

References

- [1] I.H. Hassan, M. Abdullahi, J. Isuma, S.A. Yusuf, I.T. Aliyu, A comprehensive survey of honey badger optimization algorithm and meta-analysis of its variants and applications, *Franklin Open* 8 (2024) 100141, <https://doi.org/10.1016/j.fraope.2024.100141>. July.
- [2] M. Baghoolizadeh, M. Rostamzadeh-Renani, R. Rostamzadeh-Renani, D. Toghraie, Multi-objective optimization of Venetian blinds in office buildings to reduce electricity consumption and improve visual and thermal comfort by NSGA-II, *Energy Build.* 278 (2023) 112639, <https://doi.org/10.1016/j.enbuild.2022.112639>.
- [3] R. Talami, J. Wright, B. Howard, Evaluating the effectiveness, reliability and efficiency of a multi-objective sequential optimization approach for building performance design, *Energy Build.* 329 (2025) 115242, <https://doi.org/10.1016/j.enbuild.2024.115242>. October 2024.
- [4] M. Ghaderian, F. Veysi, Multi-objective optimization of energy efficiency and thermal comfort in an existing office building using NSGA-II with fitness approximation: a case study, *J. Build. Eng.* 41 (2021) 102440, <https://doi.org/10.1016/j.job.2021.102440>. March.
- [5] Y. Lin, J. Wang, W. Yang, M. Chan, X. Hu, A case study of multi-objective design optimization of a healthy building in Shanghai, China, *J. Build. Eng.* 96 (2024) 110581, <https://doi.org/10.1016/j.job.2024.110581>. April.
- [6] W. Yu, B. Li, H. Jia, M. Zhang, D. Wang, Application of multi-objective genetic algorithm to optimize energy efficiency and thermal comfort in building design, *Energy Build.* 88 (2015) 135–143, <https://doi.org/10.1016/j.enbuild.2014.11.063>.
- [7] Z. Chen, Y. Cui, H. Zheng, Q. Ning, Optimization and prediction of energy consumption, light and thermal comfort in teaching building atriums using NSGA-II and machine learning, *J. Build. Eng.* 86 (2024), <https://doi.org/10.1016/j.job.2024.108687>. January.
- [8] Y. Wang, L. Hu, L. Hou, W. Cai, L. Wang, Y. He, Study on energy consumption, thermal comfort and economy of passive buildings based on multi-objective optimization algorithm for existing passive buildings, *J. Clean. Prod.* 425 (2023), <https://doi.org/10.1016/j.jclepro.2023.138760>. July.
- [9] G. Liu, K. Nagano, M. Ye, H. Liu, Optimization of a radiant heating system in a net Zero energy house (nZEH) to maintain a comfortable indoor environment while minimizing energy consumption, *Energy Build.* 328 (2025), <https://doi.org/10.1016/j.enbuild.2024.115208>. October 2024.
- [10] H. Cui, L. Zhang, H. Yang, Y. Shi, Optimizing thermal comfort and energy efficiency in hospitals with PCM-enhanced wall systems, *Energy Build.* 323 (2024), <https://doi.org/10.1016/j.enbuild.2024.114740>. April.
- [11] P.H. Shaikh, N.B.M. Nor, P. Nallagownden, I. Elamvazuthi, Intelligent multi-objective optimization for building energy and comfort management, *J. King Saud*

- Univ. - Eng. Sci. 30 (2) (2018) 195–204, <https://doi.org/10.1016/j.jksues.2016.03.001>.
- [12] K.R. Wagiman, M.N. Abdullah, M.Y. Hassan, N.H. Mohammad Radzi, A new metric for optimal visual comfort and energy efficiency of building lighting system considering daylight using multi-objective particle swarm optimization, *J. Build. Eng.* 43 (2021) 102525, <https://doi.org/10.1016/j.jobee.2021.102525>. April.
- [13] S.N. Makhadmeh, et al., A multi-objective grey wolf optimizer for energy planning problem in smart home using renewable energy systems, *Sustain. Oper. Comput.* 5 (2024) 88–101, <https://doi.org/10.1016/j.susoc.2024.04.001>. September 2023.
- [14] M. Dehghani, S.M. Bornapour, Smart homes energy management: optimal multi-objective appliance scheduling model considering electrical energy storage and renewable energy resources, *Heliyon* 11 (3) (2025) e42417, <https://doi.org/10.1016/j.heliyon.2025.e42417>.
- [15] M.R. Abdul Malek, N.A.A. Aziz, S. Alelyani, M. Mohana, F.N. Arina Baharudin, Z. Ibrahim, Comfort and energy consumption optimization in smart homes using bat algorithm with inertia weight, *J. Build. Eng.* 47 (2022) 103848, <https://doi.org/10.1016/j.jobee.2021.103848>. September 2021.
- [16] M.H. Sulaiman, Z. Mustafa, Using the evolutionary mating algorithm for optimizing the user comfort and energy consumption in smart building, *J. Build. Eng.* 76 (2023) 107139, <https://doi.org/10.1016/j.jobee.2023.107139>. June.
- [17] L. Bai, Z. Tan, Optimizing energy efficiency, thermal comfort, and indoor air quality in HVAC systems using a robust DRL algorithm, *J. Build. Eng.* (2024) 111493, <https://doi.org/10.1016/j.jobee.2024.111493>.
- [18] J. Sun, M. Ozawa, W. Zhang, K. Takahashi, Electricity supply chain management considering environmental evaluation: a multi-period optimization stochastic programming model, *Clean. Responsible Consum.* 7 (2022), <https://doi.org/10.1016/j.clrc.2022.100086>. November.
- [19] Y. Lu, S. Wang, Y. Zhao, C. Yan, Renewable energy system optimization of low/zero energy buildings using single-objective and multi-objective optimization methods, *Energy Build.* 89 (2015) 61–75, <https://doi.org/10.1016/j.enbuild.2014.12.032>.
- [20] K. Gao, K.F. Fong, C.K. Lee, K.K.L. Lau, E. Ng, Balancing thermal comfort and energy efficiency in high-rise public housing in Hong Kong: insights and recommendations, *J. Clean. Prod.* 437 (2024) 140741, <https://doi.org/10.1016/j.jclepro.2024.140741>. January.
- [21] R. Sharma, S. Goel, S.R. Lenka, P.R. Satpathy, Energy efficiency retrofitting measures of an institutional building: a case study in eastern India, *Clean. Energy Syst.* 7 (2024), <https://doi.org/10.1016/j.cles.2024.100111>. September 2022.
- [22] M. Marzouk, M. El-Maraghy, A. El-Shihy, M. Metawie, Evaluating energy retrofit strategies in enhancing operational performance of mosques: a case study of Al-Imam Al-Hussein Mosque, *Clean. Energy Syst.* 9 (2024), <https://doi.org/10.1016/j.cles.2024.100144>. August.
- [23] S. MacAskill, S. Becken, A. Coghlan, Engaging hotel guests to reduce energy and water consumption: a quantitative review of guest impact on resource use in tourist accommodation, *Clean. Responsible Consum.* 11 (2023), <https://doi.org/10.1016/j.clrc.2023.100156>. July.
- [24] K. Di Lu, Z.G. Wu, Multi-objective false data injection attacks of cyber-physical power systems, *IEEE Trans. Circuits Syst. II Express Briefs* 69 (9) (2022) 3924–3928, <https://doi.org/10.1109/TCSII.2022.3181827>.
- [25] H.-N. Wei, G.-Q. Zeng, K.-D. Lu, G.-G. Geng, J. Weng, MoAR-CNN: multi-objective adversarially robust convolutional neural network for SAR image classification, *IEEE Trans. Emerg. Top. Comput. Intell.* 9 (1) (2024) 1–18, <https://doi.org/10.1109/teci.2024.3449908>.
- [26] M.J. Mahmoodabadi, An optimal robust fuzzy adaptive integral sliding mode controller based upon a multi-objective grey wolf optimization algorithm for a nonlinear uncertain chaotic system, *Chaos, Solitons Fractals* 167 (2023) 113092, <https://doi.org/10.1016/j.chaos.2022.113092>.
- [27] R. Rani, R. Garg, Pareto based ant lion optimizer for energy efficient scheduling in cloud environment, *Appl. Soft Comput.* 113 (2021) 107943, <https://doi.org/10.1016/j.asoc.2021.107943>.
- [28] I. Veza, et al., Multi-objective optimization of diesel engine performance and emission using grasshopper optimization algorithm, *Fuel* 323 (2022) 124303, <https://doi.org/10.1016/j.fuel.2022.124303>.
- [29] J. Kennedy, R. Eberhart, Particle swarm optimization, in: *Proceedings of ICNN'95 - International Conference on Neural Networks 4, 1995*, pp. 1942–1948, <https://doi.org/10.1109/ICNN.1995.488968>, vol. 4.
- [30] J.H. Holland, *Adaptation in Natural and Artificial systems: An introductory Analysis With Applications to Biology, Control, and Artificial Intelligence*, U Michigan Press, Oxford, England, 1975.
- [31] Q. Zhang, H. Li, MOEA/D: a multiobjective evolutionary algorithm based on decomposition, *IEEE Trans. Evol. Comput.* 11 (6) (2007) 712–731, <https://doi.org/10.1109/TEVC.2007.892759>.
- [32] D.H. Wolpert, W.G. Macready, No free lunch theorems for optimization, *IEEE Trans. Evol. Comput.* 1 (1) (1997) 67–82, <https://doi.org/10.1109/4235.585893>.
- [33] M. Hamdy, A.-T. Nguyen, J.L.M. Hensen, A performance comparison of multi-objective optimization algorithms for solving nearly-zero-energy-building design problems, *Energy Build.* 121 (2016) 57–71.
- [34] R. Kumar, R. Singh, H. Ashfaq, Stability enhancement of multi-machine power systems using ant colony optimization-based static synchronous compensator, *Comput. Electr. Eng.* 83 (2020) 106589.
- [35] E. Hancer, A new multi-objective differential evolution approach for simultaneous clustering and feature selection, *Eng. Appl. Artif. Intell.* 87 (2020) 103307.
- [36] A. Jamali, R. Mallipeddi, M. Salehpour, A. Bagheri, Multi-objective differential evolution algorithm with fuzzy inference-based adaptive mutation factor for Pareto optimum design of suspension system, *Swarm Evol. Comput.* 54 (2020) 100666.
- [37] A.L. Bukar, C.W. Tan, L.K. Yiew, R. Ayop, W.-S. Tan, A rule-based energy management scheme for long-term optimal capacity planning of grid-independent microgrid optimized by multi-objective grasshopper optimization algorithm, *Energy Convers. Manag.* 221 (2020) 113161.
- [38] S. Mirjalili, S. Saremi, S.M. Mirjalili, L.D.S. Coelho, Multi-objective grey wolf optimizer: a novel algorithm for multi-criterion optimization, *Expert Syst. Appl.* 47 (2016) 106–119, <https://doi.org/10.1016/j.eswa.2015.10.039>.
- [39] D. Jing, J.-Q. Sun, C.-B. Ren, X. Zhang, Multi-objective optimization of active vehicle suspension system control, in: *Nonlinear Dynamics and Control: Proceedings of the First International Nonlinear Dynamics Conference (NODYCON 2019) II, 2020*, pp. 137–145.
- [40] H. Han, Y. Liu, Y. Hou, J. Qiao, Multi-modal multi-objective particle swarm optimization with self-adjusting strategy, *Inf. Sci.* 629 (2023) 580–598.
- [41] M.H. Sulaiman, Z. Mustafa, M.M. Saari, H. Daniyal, S. Mirjalili, Evolutionary mating algorithm, *Neural Comput. Appl.* 35 (1) (2023) 487–516.
- [42] M. Clerc, J. Kennedy, The particle swarm - explosion, stability, and convergence in a multidimensional complex space, *IEEE Trans. Evol. Comput.* 6 (1) (2002) 58–73, <https://doi.org/10.1109/4235.985692>.
- [43] C. Blum, A. Roli, Metaheuristics in combinatorial optimization: overview and conceptual comparison, *ACM Comput. Surv.* 35 (Jan. 2001) 268–308, <https://doi.org/10.1145/937503.937505>.
- [44] K. Deb, *Multiobjective optimization using evolutionary algorithms*. Wiley, New York, 2001.
- [45] K. Deb, L. Thiele, M. Laumanns, E. Zitzler, in: A. Abraham, L. Jain, R. Goldberg (Eds.), *Scalable Test Problems For Evolutionary Multiobjective Optimization BT - Evolutionary Multiobjective Optimization: Theoretical Advances and Applications*, Springer London, London, 2005, pp. 105–145, https://doi.org/10.1007/1-84628-137-7_6.
- [46] X.S. Yang, M. Karamanoglu, X. He, Flower pollination algorithm: A novel approach for multiobjective optimization, *Eng. Optim.* 46 (9) (2014) 1222–1237, <https://doi.org/10.1080/0305215X.2013.832237>.
- [47] L. Hou, A. Pirzada, Y. Cai, H. Ma, Robust design optimization using integrated evidence computation-with application to Orbital Debris Removal, in: *2015 IEEE Congr. Evol. Comput. CEC 2015 - Proc.*, 2015, pp. 3263–3270, <https://doi.org/10.1109/CEC.2015.7257298>. August.
- [48] Z.A. Khan, A. Khalid, N. Javaid, A. Haseeb, T. Saba, M. Shafiq, Exploiting nature-inspired-based artificial intelligence techniques for coordinated day-ahead scheduling to efficiently manage energy in smart grid, *IEEE Access* 7 (2019) 140102–140125, <https://doi.org/10.1109/ACCESS.2019.2942813>.
- [49] S. Ouyang, J. Zhou, H. Qin, X. Liao, H. Wang, A novel multi-objective electromagnetism-like mechanism algorithm with applications in reservoir flood control operation, *Water Sci. Technol.* 69 (6) (2014) 1181–1190, <https://doi.org/10.2166/wst.2013.812>.
- [50] H. Bo, Y. Nie, J. Wang, Electric load forecasting use a novelty hybrid model on the basic of data preprocessing technique and multi-objective optimization algorithm, *IEEE Access* 8 (2020) 13858–13874, <https://doi.org/10.1109/ACCESS.2020.2966641>.
- [51] S. Mirjalili, P. Jamgir, S. Saremi, Multi-objective ant lion optimizer: a multi-objective optimization algorithm for solving engineering problems, *Appl. Intell.* 46 (1) (2017) 79–95, <https://doi.org/10.1007/s10489-016-0825-8>.
- [52] V. Olgyay, *Design With Climate: Bioclimatic Approach to Architectural Regionalism*, Princeton University Press, 2015.
- [53] Z. Foroozandeh, S. Ramos, J. Soares, Z. Vale, Energy management in smart building by a multi-objective optimization model and Pascoletti-Serafini scalarization approach, *Processes* 9 (2) (2021), <https://doi.org/10.3390/pr9020257>.
- [54] O. Mayo, A century of Hardy–Weinberg equilibrium, *Twin Res. Hum. Genet.* 11 (3) (2008) 249–256.
- [55] A. Seshadri, “A fast elitist multiobjective genetic algorithm: NSGA-II, Mathlab Central, file exchange, mathworks,” pp. 1–4, 2007.
- [56] C. Coello, G. Toscano Pulido, M. Lechuga, Handling multiple objectives with particle swarm optimization, *Evol. Comput. IEEE Trans.* 8 (2004) 256–279, <https://doi.org/10.1109/TEVC.2004.826067>.
- [57] C.M. Fonseca, J.D. Knowles, L. Thiele, E. Zitzler, A tutorial on the performance assessment of stochastic multiobjective optimizers, in: *Third International Conference on Evolutionary Multi-Criterion Optimization (EMO2005)* 216, 2005, p. 240.
- [58] J.R. Schott, *Fault Tolerant Design Using Single and Multicriteria Genetic Algorithm Optimization*, Massachusetts Institute of Technology, 1995.